Organic Geochemistry 75 (2014) 151–168

Contents lists available at ScienceDirect

Organic Geochemistry

journal homepage: www.elsevier.com/locate/orggeochem

The impact of thermal maturity level on the composition of crude oils, assessed using ultra-high resolution mass spectrometry

Thomas B.P. Oldenburg *, Melisa Brown, Barry Bennett [1], Stephen R. Larter

Petroleum Reservoir Group, Department of Geoscience, University of Calgary, 2500 University Drive NW, Calgary, Alberta T2N 1N4, Canada

ARTICLE INFO

Article history:
Received 17 April 2014
Received in revised form 2 July 2014
Accepted 4 July 2014
Available online 18 July 2014

Keywords:
Thermal maturity
Crude oil
Shale oil
FTICR-MS
Polar compounds
Sulfur compounds
Nitrogen compounds
Oxygen compounds
Diamondoids
Highly alkylated diamantanes

ABSTRACT

We have examined, using a 12 Tesla FTICR-MS instrument, the impact of varying thermal maturity level on a suite of 9 related crude oils charged from source rocks covering most of the liquid petroleum generating portion of the oil window (0.68–1.11% vitrinite reflectance equivalent (%Re)). The sample suite was analyzed as whole oils under three different conditions, electrospray ionization (ESI) in positive and negative ion mode to analyze basic and acidic components, respectively, and atmospheric pressure photoionization (APPI) in positive ion mode, for sulfur and hydrocarbon species.

Increasing oil maturity level had a strong influence on the composition of all compound classes in the oils with several major observations evident:

The relative apparent abundances of all heteroatom containing compound classes detected in this study, using all ionization modes, decrease systematically with increasing oil maturation levels. Both aromatic hydrocarbons, detectable in APPI mode, and NSO compound classes (detectable in both ESI and APPI modes), as broad classes, are becoming more aromatic (shift to a greater predominance of higher DBE group members) and dealkylated (decreasing average molecular mass of individual compound groups), with increasing maturation level in the oil suite. Several putative oil maturity level dependent, molecular ratios were identified in the study. Of particular note, the relative abundance ratios of heteroatom compound classes tentatively identified as alkylated carbazoles, quinolines and benzothiophenes, compared to their benzannulated homologues are very sensitive to maturation level. Several groups of compounds show interesting and specific carbon number distributions, suggesting there may be hints of specific molecular markers in the FTICR-MS data. One observation of note is the strong increase in the relative abundance of protonated hydrocarbon components with DBE 5. We speculate this might reflect the presence of previously unreported higher molecular weight diamondoid (diamantane) species in oils with up to 40 carbon atoms or more, at advanced maturity levels. Such species may prove very valuable as molecular markers in highly mature fluids, such as those currently being produced from some shale reservoirs. Covariation of quantitative GC–MS data for alkylated hetero aromatic sulfur and nitrogen compounds in this oil suite, together with the corresponding FTICR-MS data from compounds believed to be, based on accurate mass, alkylated sulfur and alkylated nitrogen compounds, suggests that FTICR-MS already has some very rudimentary quantitation capabilities.

1. Introduction

Crude oils and extractable (solvent soluble) organic matter (EOM) fractions of source rocks are complex mixtures of chemical species derived from once living organisms and catagenetic products of kerogen maturation. Although crude oils are derived from source rock bitumens, their physical properties and chemical composition can differ significantly due to fractionations related to expulsion from the source rock (Pepper et al., 1995), secondary migration and in-reservoir processes. Advances in gas chromatography in the 1960s, and gas chromatography–mass spectrometry in the 1970s led to a quantum leap in molecular organic geochemistry. Due to their relatively high abundance in oil and their ease of analysis, the saturated and aromatic hydrocarbon fractions were the main focus of early organic geochemistry studies, with a major focus on biomarker alkanes and related aromatic compounds. As the biological markers occurred in both source rock bitumens

* Corresponding author. Address: Department of Geoscience, Faculty of Science, University of Calgary, 2500 University Drive NW, Calgary, Alberta T2N 1N4, Canada. Tel.: +1 403 2203260.
E-mail address: toldenbu@ucalgary.ca (T.B.P. Oldenburg).
[1] Current address: Schlumberger Reservoir Laboratories, Bay #2, 925, 30th Street NE, Calgary, Alberta T2A 5L7, Canada.

http://dx.doi.org/10.1016/j.orggeochem.2014.07.002
0146-6380/

and oils, they provided a tool for oil-source rock correlation, facies and maturity assessments and improved our understanding of reservoirs and petroleum migration pathways. The applications are numerous and classical petroleum geochemistry can be considered a mainstream discipline today. There remain, however, many issues, including the notion that any given petroleum in a reservoir represents not a single material derived from a single source rock at a single level of maturity, but that it is a complex integrated package of fluids contributed from multiple source rocks at multiple levels of maturity over long periods of geological time. This, together with orders of magnitude variations in crude oil component concentrations through the maturity window, inverse component concentration and maturity relationships for most biomarker species, and the ubiquitous nature of petroleum fluid mixing, means that traditional maturity and organic facies parameters are heavily compromised in many common settings (Wilhelms and Larter, 1994). New approaches are needed and with the advent of FTICR-MS (Marshall and Rodgers, 2004), it is now possible to try and extend the petroleum geochemical revolution of the late 20th century into the non-hydrocarbon species that are ubiquitously present in crude oils and in some cases, such as in an severely biodegraded oils, may be the dominant molecular species present.

The non-hydrocarbon fraction of crude oils (comprising nitrogen, sulfur and oxygen (NSO) containing organic compounds) can make up a significant proportion of petroleum. Although the importance of the heteroatom compounds has been recognized in many of the processes involved in the origin and alteration of petroleum (Tissot and Welte, 1984; Hunt, 1995), their geochemistry as a broad group, is poorly understood and few non-hydrocarbons have been used for process assessment proxies, with the exception of alkylated thioaromatics, which have been used as maturity assessment tools (Radke et al., 1982; Hughes, 1984; Radke et al., 1986; Leythaeuser et al., 1988; Radke and Willsch, 1991) and alkyl aromatic nitrogen compounds, which have been used as migration tracking tools under specific situations (Larter et al, 1996; Bechtel et al., 2013). The potential value of NSO species in migrated oils, for the definition and understanding of geochemical properties and processes such as organic facies assessment, migration, biodegradation and water washing, lies in the much greater range in physico-chemical properties exhibited by these compounds, compared to hydrocarbons and has prompted some limited research activity over the past two decades. However, these studies were restricted by the lack of suitable analytical tools (e.g., GC–MS), but recent advances, such as ultra-high resolution mass spectrometry (Fourier transform ion cyclotron resonance mass spectrometry (Marshall and Rodgers, 2004), now allow routine analysis of these often sorptive or low volatility species. While truly quantitative data are not yet available from such instruments, the instruments are sufficiently stable and data are sufficiently reproducible such that qualitative and semiquantitative analysis of processes is now possible. A first approach studying the influence of maturity on the composition of NSO heteroatom constituents of oils using FTICR-MS technology was carried out by Hughey et al. (2004). The authors compared an immature oil (0.7 %Re) (vitrinite reflectance equivalent) with a more mature oil (0.85 %Re) and observed a reduction in sulfur containing compound classes with increasing maturity. In addition, the authors suggested that thermal maturation promotes aromatization and condensation of acidic polar compounds and a decrease in the degree of alkylation. In this study, an oil suite derived from a common marine source facies with variable maturity was investigated for compositional changes in the heteroatom classes as a function of maturity level, using a 12 T ultra-high resolution mass spectrometer (FTICR-MS).

2. Samples and methods

2.1. Samples

The oil maturity suite consists of nine crude oils produced from the North Sea that belong to one single petroleum family generated predominantly in the Upper Jurassic Kimmeridge Clay Formation. As described in a previous study by Bennett et al. (2002), the maturity of these samples were defined according to proximal source kitchen temperatures and classical aliphatic and aromatic hydrocarbon maturity parameters as spanning the oil window from 0.68–1.11 $\%R_e$. Good correlations exist between the saturated and aromatic hydrocarbon and aromatic sulfur-containing species derived maturity parameters, such as Ts/(Ts + Tm) and the 4-methyldibenzothiophene/dibenzothiophene ratio, with the maturities defined according to proximal source kitchen temperature (Fig. 1). The oils were selected from reservoirs located in close proximity (< 10 km) to the source rocks to limit compositional fractionation due to secondary migration and to minimize complexity with multiple charging source rocks.

2.2. Methods

All oil samples were analyzed without fractionation using a 12 Tesla Bruker Apex Fourier transform ion cyclotron resonance-mass spectrometer (FTICR-MS) located at the Tesla Petroleomics Centre in the University of Calgary. Samples were prepared by diluting whole oils to a final concentration of 0.25 mg/ml, in a solvent composed of equal parts of toluene and methanol. Just before analysis, the samples were spiked with 1 ppm of reserpine and 1% of ammonium hydroxide for analysis in negative ion electrospray ionization (ESI-N) or 1% formic acid for analysis in positive ion electrospray (ESI-P) and atmospheric pressure photoionization (APPI-P) using a krypton lamp at 10.6 eV. The samples were introduced into the mass spectrometer using a syringe pump set to deliver 240 μl/h. The instrument was tuned and optimized using a set of standard compounds and oils and calibrated daily. Internal standards are included in each sample suite to ensure mass accuracy. Typically, for each sample, 200 scans are collected and summed to improve the experimental signal/noise ratio. For a typical crude oil sample the mass range of the instrument is set to between 165.88 Da and 1400.00 Da.

The resolving power at 400 Da is > 500,000 (M/ΔMfwhm). The mass accuracy is typically < 200 ppb.

The data were processed by recalibration with known oil constituents and each species assigned to chemical molecular formulae, mainly as CcHhNnSsOo compounds, using the Composer software (Sierra Analytics). Ragnarök (Aphorist Inc.), a data processing software tool for quantitation, visualization and interpretation of multidimensional and multi-sample FTICR-MS data was then used for the data analysis and visualization. Apart from the determination of molecular masses and double bond equivalents (DBE derived as DBE (CcHhNnSsOo) = $c - h/2 + n/2 + 1$) of detectable individual species in whole oils or bitumen fractions (see the definitions below), we derived lumped abundances of whole heteroatom classes (a heteroatom class is a group of compounds with a uniform heteroatom population), DBE group distributions within a heteroatom class, carbon number distributions of an individual group of pseudohomolog compounds and also a variety of plots, including modified Kendrick plots and averaged molecular mass plots for related groups of compounds. The terminology we use in this paper is defined in the chart in Appendix A.

3. Results

The number of detectable compound classes using FTICR-MS strongly decreases with increasing maturity when analyzed as whole oils under identical conditions (Table 1). "Identical conditions" indicates that during analysis, the same volume of oil and dopant with the same concentration of the whole oil and dopant were injected, the same number of scans and other FTICR-MS specific settings were maintained constant. For low maturity samples, 15 compound classes are easily identified above the detection limit using ESI-N and APPI-P and 8 in ESI-P mode. In the most mature oil sample (1.11 %Re), only 6 compound classes are detected using each ionization mode. There is certainly an overlap between the compound classes measured in the three different ionization modes, e.g. the N_1 class is detected in all three ionization modes reflecting mainly pyrroles (ESI-N), pyridines (ESI-P) and probably both of these structures in APPI-P as PRO and RAD ions. However, as we do not know at this stage how much overlap exists between the different compound classes we are considering here for counting of the number of compound classes for each ionization mode separately, e.g. N_1 class is counted as 4 classes. With this, a reduction of the total number of compound classes across all ionization modes, from 38 to 18 with increasing maturity (see Table 1), likely mirrors the progressive elimination of functional groups from the kerogen during maturation and also the dilution of nonhydrocarbons by hydrocarbons, as maturation proceeds. A general decrease in compound classes at higher levels of maturity was also reported in a previous study (Hughey et al., 2004). At high maturity, only the most stable heteroatom moieties incorporated directly into the molecular ring systems are left to be released from the kerogen. Despite the reduction in the number of compound classes with increasing maturity, the most dominant class seen in each ionization mode was retained throughout the oil sample suite. The analyses with the ESI ionization technique revealed the dominance of nitrogen-containing compounds in both positive and negative ionization modes. Alkylated pyridines (N_1 class) dominate in ESI-P mode, but the proportion of these species decreased with increasing maturity, from 86% at 0.7 %Re to 63% at 1.1 %Re of the total ion response. Pyrrolic species (N_1 class) dominate in ESI-N mode and similarly decrease from 62% to 40% of the total ion response. In addition, an increase in the percentage of total hydrocarbons was observed, as the most dominant species identified in APPI-P, with increasing maturity. The relative intensities of hydrocarbons relative to total ion current increased from 50% to 92% over the range of oil maturity investigated. Total hydrocarbon class (HC total) is defined as the sum of all radical (HC RAD) and all protonated (HC PRO) hydrocarbon ions. Whereas the HC RAD component increased from 38% to 66% of total ion current, the HC PRO increased from 12% to 26% over the investigated oil maturity range. Simultaneously, the abundance of the S_1 class, the second most intense compound class in APPI-P, decreases with increasing maturity from 28% to 1% of total ion current.

3.1. Pyrrolic N_1 class (measured in ESI-N mode)

Previous studies of pyrrolic species in petroleum were limited to low molecular weight alkylated carbazoles, benzo- and dibenzocarbazoles, with less than three alkyl carbon substituents due to the analytical restrictions of GC–MS (Larter et al., 1996). Pyrrolic nitrogen species are ubiquitous components of crude oils and source rock extracts (Helm et al., 1960; Frolov et al., 1989). The biological origins of those compounds remain unclear. Their precursors have been traced to alkaloids, proteins and pigments in algae and terrigenous plants (Snyder, 1965; Hesse, 1974), although thermal maturation processes in source rocks undoubtedly generate a wide variety of aromatic heteroatomic species from a variety of non-specific precursors.

The N_1 heteroatom class analyzed with the ESI-N ionization mode technique is dominated by alkylated pyrrolic constituents and other "deprotonatable" (acidic) nitrogen species. The distributions of the N_1 class species analyzed in ESI negative ion mode that are found in the maturity oil suite are displayed by DBE group as two different line plots of species abundance by intensity (Fig 2I), and fraction of class (Fig. 2II). These two illustrations allow us to derive different information regarding compositional changes in the oils with maturity. For instance, the intensity plot (Fig. 2I) permits an estimation of the relative apparent concentration changes of the DBE groups in the whole oils. The intensity is a measure of relative abundance as the sample amount infused into the source and the instrument settings and analytical conditions are kept unchanged from sample to sample. A relative decrease in total N_1 species with increasing oil maturity is reflected by this plot. Fig. 2I indicates that the relative concentration of the low DBE group members (including likely alkylated carbazoles and benzocarbazoles) of the N_1 heteroatom class, first slightly increases with increasing oil maturity (0.68 %Re to 0.75 %Re), followed by a relative decrease in relative abundance at higher maturity. A strong decrease in the relative concentration of all N_1 class constituents is observed with increasing oil maturity, especially for the samples with maturities between 0.85 %Re to 1.11 %Re. Also seen as a trend, is a reduction in the total number of detectable DBE groups of compounds with increasing oil maturity. This suggests that non-hydrocarbon compositional spectra are becoming simpler with increasing maturity in crude oils, which is not unexpected. Previous studies of oils with GC–MS technology by Clegg et al. (1998) revealed that the concentration of carbazole and methylcarbazoles increased with maturity (0.5–0.9 %Re) for oils from the Sonda de Campeche Basin, but no increase in the concentration of non-alkylated benzocarbazole compounds with maturity was observed. The concentrations of the non-alkylated carbazole, benzocarbazoles and methylcarbazoles analyzed for Tithonian source rocks from the same area were reported to, at first, slightly decrease with increasing maturity (0.3–0.8 %Re), followed by an increase in concentration to a peak abundance at 1.1 %Re, with a strong subsequent reduction in concentration of carbazole species towards 1.3 %Re. The diverging trends seen for carbazole and methylcarbazoles concentrations for the oils and source rocks was interpreted by the authors as indicative of expulsion of those compounds throughout a broad range of maturity. The increase in concentrations between 0.8 %Re and 1.1 %Re was thought to be related to further generation of the species from kerogen in the source rocks.

Bennett et al. (2002) reported on the alkylated carbazole systematics for the same oil maturity sample suite as studied in this article. They observed, firstly a decrease in the non-alkylated benzocarbazole isomer concentrations (benzo(a)carbazole + benzo(c)carbazole), over the oil maturity range 0.68–0.78 %Re. This initial decrease in benzocarbazole concentrations was suggested by the authors to be related to a stage of dilution of initial benzocarbazole levels by more rapidly generated petroleum species prior to release from the source rock. A 4-fold increase in benzocarbazole concentrations was observed near 0.8 %Re, followed by a strong decrease in concentration towards an oil maturity level near 1.1 %Re. The maximum concentrations of benzocarbazoles seen in the oils at a maturity level of 0.85 %Re were similar to those seen in North Sea, Jurassic age, Kimmeridge Clay Formation source rocks reported in the same article at a maturity level of 0.7–0.75 %Re. This was similar to the observations of Clegg et al. (1998).

It is difficult to make a direct comparison between observations made on the North Sea oil suite using GC–MS, where only the non-alkylated (C0) benzocarbazoles were analyzed (Bennett et al., 2002), and FTICR-MS, where the DBE12 group of the N_1 class likely

Table 1
Absolute intensities of compound classes analyzed with different ionization techniques (atmospheric pressure photoionization in positive ion mode (APPI-P) producing radical ions (RAD) and protonated ions (PRO), electrospray ionization in positive ion mode (ESI-P) producing protonated ions (PRO) and electrospray ionization in negative ion mode (ESI-N) producing de-protonated ions (DPR)). The dashes reflect compound classes not detected (see Appendix A for definition). The numbers in the top row reflect the maturity of the oil samples in vitrinite reflection equivalents (%Re).

%Re	0.68				0.74				0.75a				0.75b				0.78				0.84a				0.84b				0.85				1.11			
	APPI-P		ESI-P	ESI-N	APPI-P		ESI-P	ESI-N	APPI-P		ESI-P	ESI-N	APPI-P		ESI-P	ESI-N	APPI-P		ESI-P	ESI-N	APPI-P		ESI-P	ESI-N	APPI-P		ESI-P	ESI-N	APPI-P		ESI-P	ESI-N	APPI-P		ESI-P	ESI-N
	RAD	PRO	PRO	DPR	RAD	PRO	PRO	DPR	RAD	PRO	PRO	DPR	RAD	PRO	PRO	DPR	RAD	PRO	PRO	DPR	RAD	PRO	PRO	DPR	RAD	PRO	PRO	DPR	RAD	PRO	PRO	DPR	RAD	PRO	PRO	DPR
HC	10.00	2.96	–	–	14.70	4.54	–	–	14.23	4.59	–	–	16.22	4.79	–	–	11.26	3.39	–	–	13.88	3.86	–	–	12.35	3.53	–	–	12.44	4.32	–	–	4.68	1.90	–	–
N	1.73	0.28	19.85	10.83	2.55	0.39	18.83	15.61	1.94	0.29	19.72	14.43	2.76	0.39	13.33	11.21	0.81	0.08	16.48	6.74	1.36	0.14	18.47	11.78	1.03	0.07	17.97	10.01	1.14	0.11	18.90	9.95	0.08	–	6.98	0.58
NO	0.27	0.31	1.15	2.18	0.38	0.38	1.11	2.75	0.41	0.21	1.32	3.66	0.30	0.39	0.57	1.27	–	–	1.12	1.00	–	–	1.58	2.10	–	–	1.76	2.04	–	–	1.29	1.49	–	–	1.26	0.07
NO_2	–	–	–	0.99	–	–	–	0.79	–	–	–	1.28	–	–	–	0.37	–	–	–	0.25	–	–	–	0.74	–	–	–	0.73	–	–	–	0.56	–	–	–	–
NO_3	–	–	–	0.47	–	–	–	0.31	–	–	–	0.61	–	–	–	–	–	–	–	–	–	–	–	0.34	–	–	–	0.35	–	–	–	0.26	–	–	–	–
NS	–	–	1.36	0.58	–	–	1.43	1.13	–	–	1.28	0.88	–	–	0.82	0.71	–	–	0.93	0.29	–	–	0.67	0.46	–	–	0.64	0.34	–	–	0.22	0.14	–	–	0.10	–
N_2	–	–	0.38	0.16	–	–	0.34	0.20	–	–	0.25	–	–	–	0.13	0.11	–	–	0.10	–	–	–	0.27	0.10	–	–	0.19	–	–	–	0.16	–	–	–	–	–
NOS	–	–	–	0.21	–	–	–	0.28	–	–	–	0.29	–	–	–	–	–	–	–	–	–	–	–	–	–	–	–	–	–	–	–	–	–	–	–	–
NaOS	–	–	0.21	–	–	–	0.55	–	–	–	0.55	–	–	–	0.44	–	–	–	0.89	–	–	–	0.39	–	–	–	0.51	–	–	–	0.13	–	–	–	0.19	–
NaO_2S_2	–	–	0.27	–	–	–	0.72	–	–	–	1.15	–	–	–	0.27	–	–	–	–	–	–	–	–	–	–	–	–	–	–	–	–	–	–	–	–	–
O	1.94	0.54	–	3.46	2.36	0.73	–	3.34	2.48	0.81	–	2.76	2.12	0.70	–	2.83	1.75	0.58	–	1.93	2.08	0.51	–	4.45	2.03	0.51	–	3.03	1.45	0.40	–	4.45	0.32	0.11	–	0.24
O_2	0.25	0.07	–	2.26	0.27	0.11	–	2.01	0.35	0.14	–	2.41	–	–	–	0.98	–	–	–	1.70	0.18	–	–	1.94	–	–	–	2.10	–	–	–	2.35	–	–	–	0.34
O_3	–	–	–	0.79	–	–	–	0.12	–	–	–	0.67	–	–	–	–	–	–	–	0.16	–	–	–	0.33	–	–	–	0.52	–	–	–	0.31	–	–	–	0.13
O_4	–	–	–	0.45	–	–	–	0.09	–	–	–	0.49	–	–	–	–	–	–	–	–	–	–	–	0.34	–	–	–	0.48	–	–	–	0.28	–	–	–	0.09
OS	0.19	0.70	0.69	0.23	0.43	0.93	1.00	0.34	0.51	0.77	0.91	0.34	0.37	0.70	0.39	0.23	0.17	0.46	2.35	0.12	0.11	0.36	2.16	0.21	0.09	0.28	2.36	0.14	–	–	1.21	–	–	–	2.58	–
O_2S	–	–	–	0.30	–	–	–	0.38	–	–	–	0.37	–	–	–	0.16	–	–	–	0.11	–	–	–	0.19	–	–	–	0.13	–	–	–	–	–	–	–	–
O_3S	–	–	–	0.49	–	–	–	0.50	–	–	–	0.42	–	–	–	0.15	–	–	–	0.20	–	–	–	0.35	–	–	–	0.22	–	–	–	0.11	–	–	–	–
O_4S	–	–	–	0.38	–	–	–	0.31	–	–	–	0.35	–	–	–	0.23	–	–	–	–	–	–	–	–	–	–	–	–	–	–	–	–	–	–	–	–
O_2S_2	–	–	–	–	–	–	0.22	–	–	–	0.23	–	–	–	0.07	–	–	–	–	–	–	–	–	–	–	–	–	–	–	–	–	–	–	–	–	–
S	4.49	1.40	–	–	8.32	2.48	–	–	7.11	2.06	–	–	8.31	2.36	–	–	4.17	1.20	–	–	3.35	0.77	–	–	2.75	0.58	–	–	0.85	0.11	–	–	0.09	–	–	–
S_2	–	–	–	–	0.61	–	–	–	0.40	–	–	–	0.51	–	–	–	0.17	–	–	–	–	–	–	–	–	–	–	–	–	–	–	–	–	–	–	–

The intensities are in 1E+10.

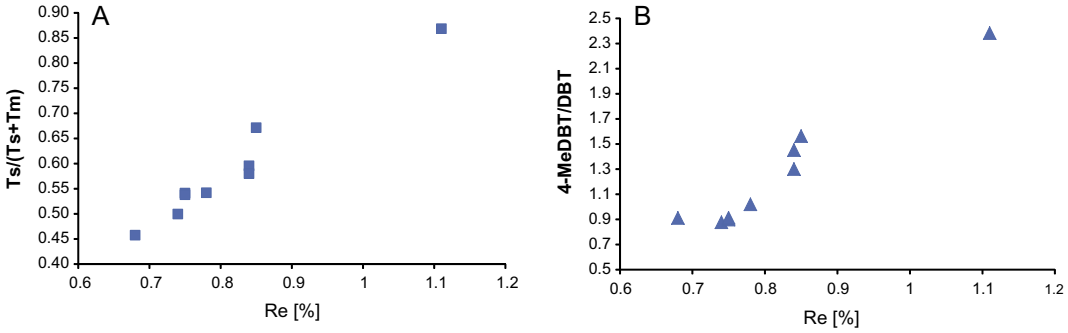

Fig. 1. Plots of molecular maturity parameters (A) Ts/(Ts + Tm) and (B) 4-methyldibenzothiophene (4-MeDBT)/dibenzothiophene (DBT) ratio relative to the vitrinite reflectance equivalent (Re%) of the putative source rock interval in the studied oil maturity suite. (After Bennett et al. (2002).)

represents alkylated benzocarbazoles with alkyl chains from C3 to C34. N_1 DBE12 species corresponding with 0–2 alkyl carbons were not detected, most likely due to lower sensitivity of FTICR-MS at low mass. Overall, higher oil maturity (0.85–1.11 %Re), results in a reduction in the relative concentration of benzocarbazole species seen by FTICR-MS corresponding to similar reductions in the concentration of the carbazole fraction seen by GC–MS. Thus, while it seems plausible to believe that higher molecular weight benzocarbazole species will respond in a similar manner as low molecular weight benzocarbazole species, this is not proven by FTICR-MS. What can be stated is that the entire N_1 heteroatom class (likely, mostly carbazole type compounds), shows a reduction in the relative concentration compared to other compound types with increasing oil maturity and this reflects a general process of dealkylation of aromatic and heteroatom pseudohomologs with increasing maturity levels.

The second main graph (Fig. 2II) illustrates the normalized distribution of the N_1 heteroatom class by DBE measured in ESI negative ion mode. That is, the sum of intensities of all detected N_1 class species is normalized to one. This illustration reveals more clearly the compositional changes that correspond to increasing oil maturity within the N_1 class. Considering just the N_1 species with DBE 9, which most likely are associated with alkylated carbazoles, their relative abundance can be clearly seen decreasing with increasing oil maturity. Simultaneously, with the relative depletion of the DBE 9 group concentrations, N_1 heteroatom class components with DBE numbers > 12 are seen to be increasing, on a relative basis, with increasing oil maturity, especially for the summed pseudohomologs of the DBE 15 group. The compounds with DBE 15 are unidentified, but we speculate are most probably alkylated dibenzocarbazoles. However, the carbon number range of the three related groups with DBE 9, 12 and 15 (likely carbazoles [C], benzocarbazoles [BC], and dibenzocarbazoles [DBC]), reveals a similar decrease in the number of pseudohomologs seen within each DBE group with increasing maturity level. Thus, the number of pseudohomologs decreases from 30 to 15 for DBE 9 (carbazoles), from 31 to 18 for DBE 12 (benzocarbazoles) and from 31 to 17 for DBE 15 (di benzocarbazoles) over the range of oil maturity within the sample set (see graphs in Fig. 5). This suggests that a general oil maturity related dealkylation process is common, throughout many different heteroatom DBE groups of compounds.

The graphs showing pseudohomologs C# distribution of different DBEs in Fig. 5 indicate that the oil at mid oil window maturities (0.78 %Re) has a slightly different distribution profile, with higher concentrations of C_{30}–C_{38} pseudohomologs, relative to all the other oils. In addition, the ratio of the abundances of pseudohomologs with DBE 9 (likely alkylated carbazoles) to the species with DBE 10 in this sample is higher than in the other samples. This might indicate that this oil is at least partially charged from a second source, or at least reflects some local variation in the source rock charging the oils.

The oil maturity related changes within the N_1 heteroatom class become more obvious when plotted in a triangular diagram showing the relative changes of the three major compound groups (likely carbazoles (DBE 9), benzocarbazoles (DBE 12) and dibenzocarbazoles (DBE 15)) relative to each other with oil maturity (Fig. 3). With increasing oil maturity, the N_1 heteroatom class becomes increasingly dominated in relative abundance, by the more benzannulated species. The generally linear relationship between oil maturity and the position of individual oil samples within the DBE 9, 12 and 15 space on the diagram, suggests that variations between these three N_1 heteroatom DBE groups might be developed as a maturity assessment tool. In addition, in the highest maturity oils, highly condensed constituents with 14 DBEs (possibly alkylated pyrenopyrroles, 4H-naphtho[1.2.3.4-def]carbazoles or fluorenoisoindoles), which are even more condensed than the dibenzocarbazoles also increase in relative abundance (Fig. 2). Our previous studies have shown that biodegradation strongly influences the distribution of C0–C2 alkylated homologs of these compound groups (Huang et al., 2003; Oldenburg, 2004; Oldenburg et al., 2006), but that the higher molecular weight homologs are likely to be quite biodegradation resistant (Larter et al., 2013; Oldenburg et al., 2013). In addition, the influence of source facies on the distribution of nonhydrocarbon species has to be defined and we will comment on the source facies controls on the polar fractions of crude oils, in part two of this series.

Fig. 4 shows the changes in the average molecular mass per DBE group and for the entire N_1 heteroatom class (embedded graph), with increase in oil maturity for the North Sea oil sample set. An overall reduction in the averaged molecular mass (AMM) of the whole N_1 heteroatom class of about 12 Da, was observed with increasing oil maturity level for this sample set (Fig. 4, small embedded diagram). Note: two oils with maturities of Re 0.78% and 0.85%, show slightly higher AMM values. Clearly this is a small data set and the change in AMM is small but this likely reflects the common trend of dealkylation and molecular weight decrease with increasing maturity. The main diagram of Fig. 4 shows more detail of the changes in the molecular weight distribution of the N_1 heteroatom class for different DBE groups. The difference in averaged molecular mass per DBE group, between the least mature to the most mature oil sample, increases with increasing DBE from around 5 Da over the full range of oil maturity (0.7–1.1 %Re), at DBE 10, up to a 43 Da difference across the full range of oil maturity, with more aromatic and larger ring number pseudohomologs, e.g. as seen at DBE 21, 22. The generally lower averaged molecular mass, for any DBE group at higher oil maturity levels (e.g. 1.11 %Re), is likely related to progressive dealkylation of all aromatic and heteroatomic species with increasing oil maturity. The AMM

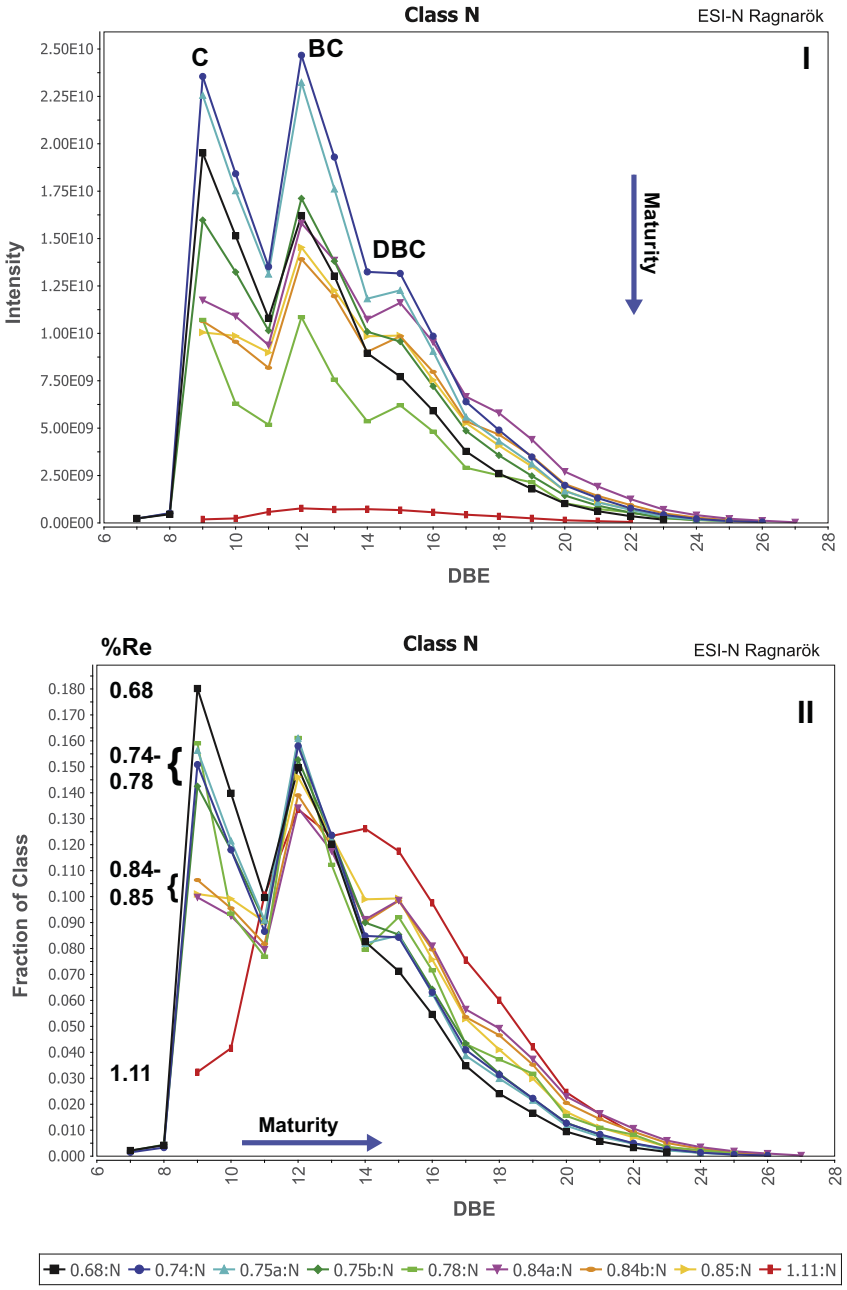

Fig. 2. Distribution of N_1-class (probably pyrrolic, nitrogen species) measured in ESI negative ion mode. The three plots show the distributions of these molecular types, sorted into groups of double bond equivalent pseudohomologs (DBE). Data is displayed in three ways: I. As an ion "Intensity" plot (of each individual DBE group of compounds, plotted versus DBE number); II. As a "Fraction of Class" plot (sum of the intensities of all components within one DBE group normalized to the sum of all assigned peak abundances of one (heteroatom) class measured in one ionization mode. N_1 class DBE 9 group pseudohomologs are most likely dominantly alkylated carbazoles (C), based on abundant evidence of these species being dominant components in the lower carbon number regions accessible by GC MS studies, whereas DBE 12 group species are likely predominantly benzocarbazoles (BC) and DBE 15 group species are likely largely dibenzocarbazoles (DBC). [The numbers to the left of the diagram II. indicate the oil maturity assessed as vitrinite reflectance equivalent (%Re).] The numbers and symbols shown in the legend at the bottom of all figures reflect the maturity level of each oil sample, reported as %Re.

changes between the different DBE group pseudohomologs of the N_1 heteroatom class can also indicate structural information, to some limited extent. For instance, the AMM versus DBE profile for the N_1 heteroatom class, shows the lowest AMM values for compound groups with DBE 9, 12, 15, 18 and 21, when compared to the abundances of compounds in other DBE groups near to them (e.g., DBE 10–11, 13–14, 16–17, 19–20 compound classes). The DBE 9, 12, 15, 18 and 21 groups represent pseudohomologs with likely fully aromatic core structures, such as carbazoles and the benzannulated compounds, whereas other DBE groups are likely to contain saturated rings in addition to the alkylated aromatic nitrogen bearing core. This pattern changes at high oil maturity, particularly for the oil with highest maturity (1.11 %Re). For example, compounds with DBE 11 contain a similar AMM compared to the benzocarbazoles (DBE 12) and DBE 13 and 14, similar to dibenzocarbazoles (DBE 15). While speculative, this may indicate that for instance DBE 11 compounds, are now dominated by fully aromatic cored systems, such as dibenzo[def]carbazoles or iminophenanthrenes, rather than having saturated rings attached to an aromatic core. Similar changes suggesting evolution of heteroatom ring systems

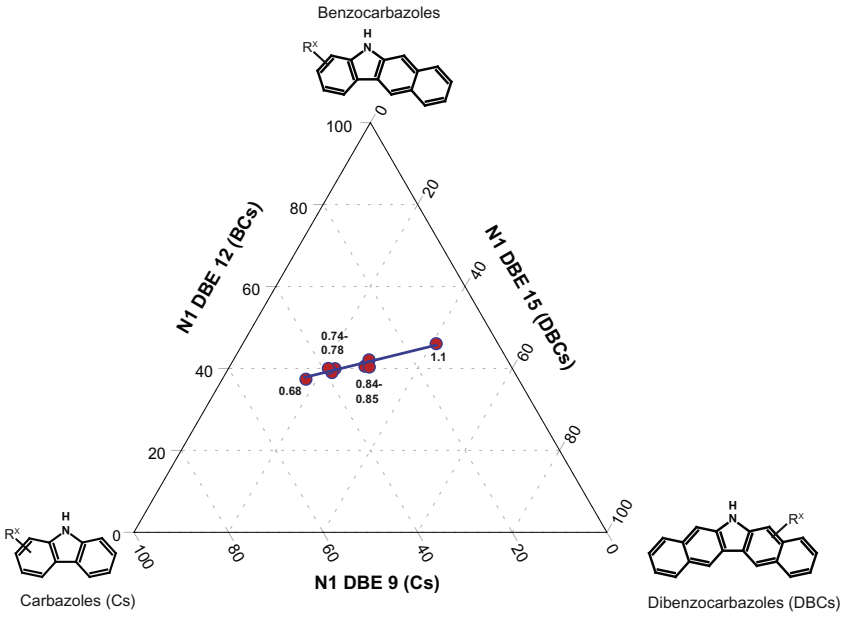

Fig. 3. Triangular plot illustrating the effect of maturity changes on the relative distribution of DBE 9 (likely alkylated carbazoles), DBE 12 and 15 (likely alkylated benzo- and alkylated dibenzocarbazoles, respectively). [Numbers indicate the oil maturity assessed as vitrinite reflectance equivalent (%Re); molecular structures illustrate possible core structures that correspond to a specific DBE number and compound group.]

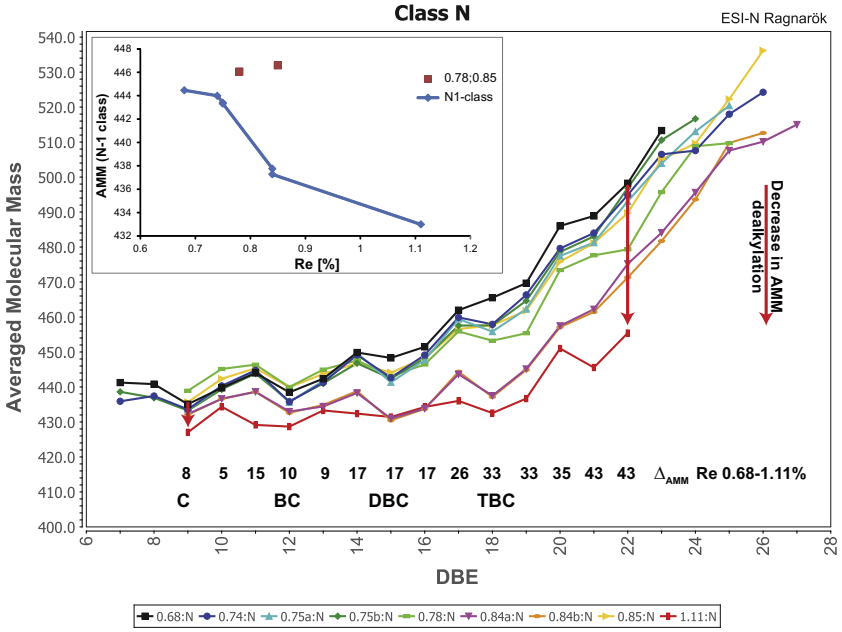

Fig. 4. Averaged molecular mass (AMM) for each DBE group of the N_1 heteroatom class measured in ESI negative ion mode. DBE 9 group compounds are likely alkylated carbazoles (C), DBE 12 group compounds are likely benzocarbazoles (BC), DBE 15 compounds are likely alkylated dibenzocarbazoles (DBC) and DBE 18 compounds are likely alkylated tribenzocarbazoles (TBC). [Numbers below the trace lines indicate the mass difference per DBE between the least mature (0.68 %Re) and the most mature oil (1.11 %Re) sample for each DBE group.] The small embedded diagram illustrates the averaged molecular mass of the N_1 heteroatom class versus maturity (%Re) for all oil samples. The numbers in the bottom key indicate the vitrinite reflectance equivalents of the range of oils of different maturities. The two slightly anomalous oil sample data are plotted with red squares. (For interpretation of the references to color in this figure legend, the reader is referred to the web version of this article.)

towards fully aromatic molecule cores (AMC) with increasing oil maturity are observed for the higher DBE groups, too. This becomes clearer when looking at the changes in the distribution pattern and the relative abundances of carbazoles and their benzannulated homologs with increasing maturity level (Fig. 5).

As described earlier, the relative abundance of the carbazoles in oils decreases with increasing level of oil maturity. However, for the higher benzannulated homologues, this trend reverses on a relative basis within the heteroatom class. Furthermore, the distribution patterns of the DBE 18 and 21 groups clearly show an increase in the relative abundance in the lower pseudohomolog carbon number range for the samples at high oil maturity level (0.84 %Re and 1.11 %Re). This again, is possibly related to a relative increase in components with fully aromatic compound cores as oil maturity increases. The molecular structures shown in Fig. 5, illustrate a few possible non-alkylated moieties that might be

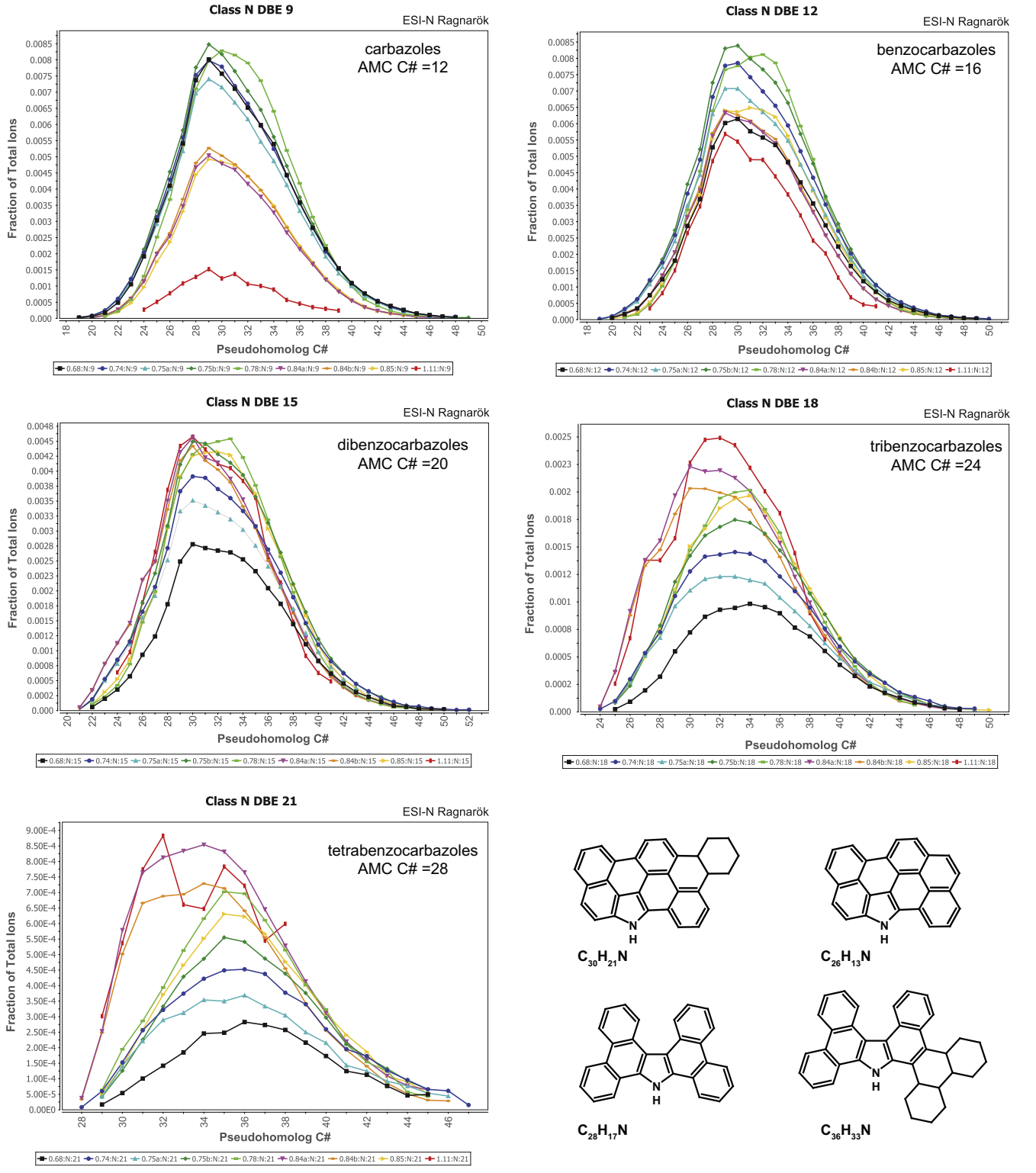

Fig. 5. Distribution of DBE 9, 12, 15, 18 and 21 compound groups of the pyrrolic N_1 heteroatom class (likely carbazoles (C) and their benzannulated homologues benzo-, dibenzo-, tribenzo- and tetrabenzocarbazoles) sorted by pseudohomolog carbon number C# versus the fraction of the total heteroatom class (sum of intensities of all pseudohomolog C# of all DBE groups is 1) measured in ESI negative ion mode. [AMC C# stands for aromatic molecular core carbon number, i.e. the C# of the non-alkylated aromatic molecule.] The numbers in the bottom key indicate the vitrinite reflectance equivalents of the range of oils of different maturities. The molecular structures illustrate four possible different cyclic cores of the DBE 21 group of compounds with 26, 28, 30, and 36 carbon atoms.

representative for compounds in the N_1 heteroatom class DBE 21 group. The structures are illustrative for components with different numbers of carbons in the core ring system (C# = 26, 28, 30, 36). It is of course important to remember, that many equivalent structures are possible. It seems likely that substantially dealkylated and highly aromatic heteroatom species become more abundant in crude oil polar fractions as oil maturity increases. Even more condensed compounds (e.g., with 26 carbons) compared to

tetrabenzocarbazoles (28 carbons) are likely at DBE 21. The overall increase in DBE can only be plausibly explained by aromatization and/or condensation reactions and the carbon number range reduction reflects the dealkylation associated with increasing oil maturity.

3.2. O_1 heteroatom class (measured in ESI-N mode)

O_1 species are the second most abundant heteroatom class analyzed by ESI-negative ionization. The detected O_1 species are most likely components with a hydroxyl functional group able to be deprotonated. Fig. 6A and B shows the O_1 heteroatom class distribution in a modified Kendrick plot of the least (0.68 %Re equivalent) and most mature (1.11 %Re equivalent) oil samples, respectively. A strong apparent relative reduction in the number of detectable pseudohomologs is observed for the higher maturity oil sample, compared to its lower maturity family member. Of note, we see that non-aromatic compounds (with DBE 1–3), and highly alkylated compounds (carbon number > 38) are absent, at this level of detection, in the most mature oil sample. Fig. 6C shows the strong reduction in the relative abundance of the O_1 heteroatom class DBE 5 group pseudohomologs with increasing oil maturity. This may partly reflect the reduced quantity of organic oxygen compounds that can be released incrementally from the source rock kerogen at these elevated levels of maturity and partly be due to the thermal decomposition of such free species prior to migration. Source temperatures well in excess of 150 °C are inferred at 1.1 %Re. In addition, the components that are released from kerogens at higher maturity levels are more aromatic and less alkylated compared to those sourced from less mature kerogens. The strong predominance of compounds with 27 carbon atoms (C_{27}), especially seen in the data for the lower maturity oil samples, is of note. Steroidal compounds and especially steranes, are common constituents of petroleum (mainly C_{27}–C_{29}, Mackenzie et al., 1982), with a predominance of the C_{27} homologues for marine sourced oils. Sterols, with a hydroxyl functional group present such as cholesterol, are not commonly reported in crude oils, so it is unclear what the strong electrospray negative mode signal indicating a single oxygen atom containing compound at C_{27} actually is. It seems unlikely that sterols are actually present in the oils and contamination is always a worry, though we have actually isolated sterols from some very severely biodegraded oils (unpublished work with D.M. Jones, Newcastle University). These observations remind us that FTICR-MS on its own cannot be used to reliably identify specific compound types and therefore, we need to be very cautious in terms of even tentative identification of these species. Further classical liquid chromatography and GC–MS work is clearly needed, but the value of FTICR-MS as a reconnaissance tool for potentially interesting molecular markers is clearly evident. The oil with intermediate maturity (0.78 %Re) is, in addition, somewhat enriched in compounds with 28 carbon atoms, unlike the main suite of samples, which again might indicate that this oil is at least partially charged from a second source or reflects a contribution from a local facies variation in the source rock.

3.3. N_1 heteroatom class (measured in ESI-P mode)

Alkylated pyridines and their benzannulated homologs are known to be constituents of fossil fuels (Ball, 1962; Snyder, 1970; Patience et al., 1992; Li et al., 1992; Oldenburg et al., 2004, 2007). The origin of such pyridinic and related compounds is not known, but pyridine derivatives are often part of biomolecules such as alkaloids and nucleotides (e.g., Newkome, 2008). The response of the mass spectrometer to the N_1 heteroatom class, measured in ESI-P mode, reflects the protonation potential of the species being analyzed. Similar general trends in alkylation level, aromatic core ring size and other features are seen in the N_1 heteroatom compound class, measured in ESI-P mode, with varying oil maturity, as are seen with the N_1 heteroatom class analyzed by ESI-N mode. Oils at low maturity levels (0.68–0.75 %Re) are dominated by DBE 7 and 10 likely quinolines and benzoquinolines, respectively, among other pseudohomologs (Fig. 7). At moderate levels of maturity (0.78–0.85 %Re), benzoquinolines and pseudohomologs (DBE 10), with a more full aromatic core structure are seen to become predominant within the heteroatom class. This is changing at high levels of maturity (1.11 %Re), in favor of a relative increase in the apparent abundance of compounds having 12 DBEs with likely a very robust aromatic core structure which might be indenoquinolines or azopyrenes, though this is not confirmed.

Fig. 8 illustrates the remarkable changes seen between the 2 ring aromatic components at DBE 7 (likely, alkylated quinolines) and the DBE 12 constituents (possibly alkylindeno-quinolines and/or -azopyrenes). Whereas quinolines (DBE 7) are clearly decreasing in relative abundance with increasing oil maturity level, the DBE 12 species appear to increase in relative abundance with increasing maturity level. This once again, indicates an apparent shift to more abundant, on a relative basis, more condensed aromatic structures, in the polar fraction of the oils with increasing maturity level. This trend is well illustrated in a triangular diagram of the relative distribution of putative alkylated quinolines (DBE 7), alkylated benzoquinolines (DBE 10) and DBE 13 (alkylated dibenzoquinolines) or DBE 12 (alkylated indenoquinolines or azopyrenes). Figs. 9 and 10, show, in a similar manner to the corresponding N_1 heteroatom group constituents (DBE 9, 12 and 15 detected in ESI-N mode), seen

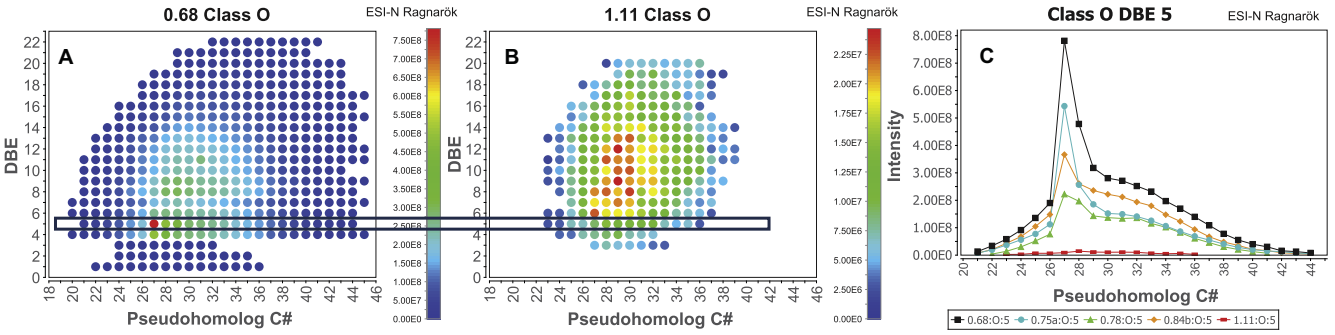

Fig. 6. Modified Kendrick plots of O_1-heteroatom class (probably hydroxylated compounds) of the least mature oil (A), and most mature oil (B), are shown with the DBE 5 group components highlighted [color indicates intensities normalized to the most abundant pseudohomolog within the heteroatom class. Graph C illustrates the distribution of the DBE 5 group of the O_1 class sorted by pseudohomolog C# versus peak height abundance measured of selected oils (0.68, 0.75, 0.78, and 1.11 %Re) in ESI negative ion mode. The numbers in the bottom key of graph C indicate the vitrinite reflectance equivalents of the range of oils of different maturities. (For interpretation of the references to color in this figure legend, the reader is referred to the web version of this article.)

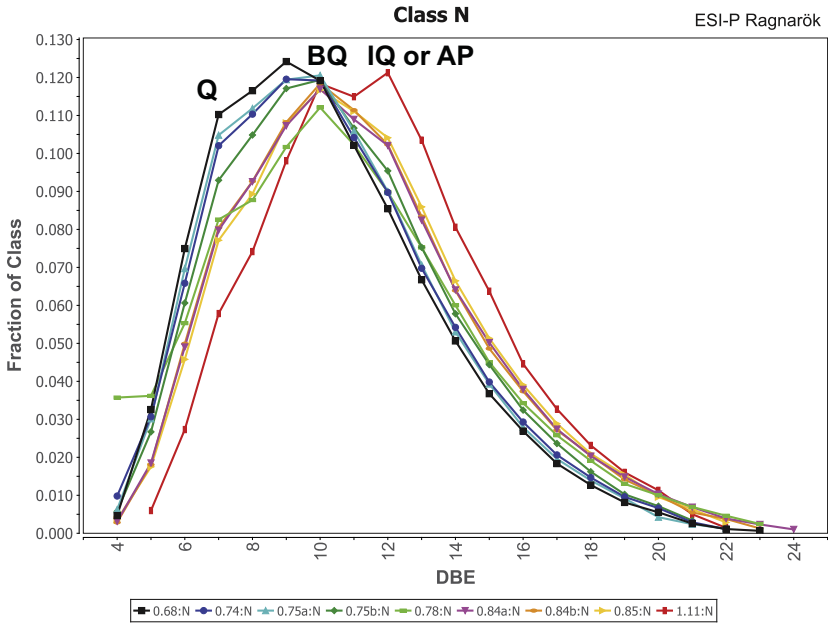

Fig. 7. Distribution of N_1 heteroatom class compounds (likely alkylated pyridinic species based on the common occurrence in crude oils: Li et al., 1992) sorted as groups of species with common double bond equivalents (DBE) and plotted versus the fraction of the total heteroatom class ion response (sum of intensities of all DBE groups of the heteroatom class is 1) of each DBE compound group, measured in ESI positive ion mode. The DBE 7 group of pseudohomologs is possibly quinolines (Q), the DBE 10 group of components are the benzoquinolines (BQ) and the DBE 12 group of pseudohomologs might be indenoquinolines (IQ) or azopyrenes (AP). The numbers in the bottom key indicate the maturity levels of the range of oils in this sample suite, expressed in terms of vitrinite reflectance equivalent for the source rock (%Re).

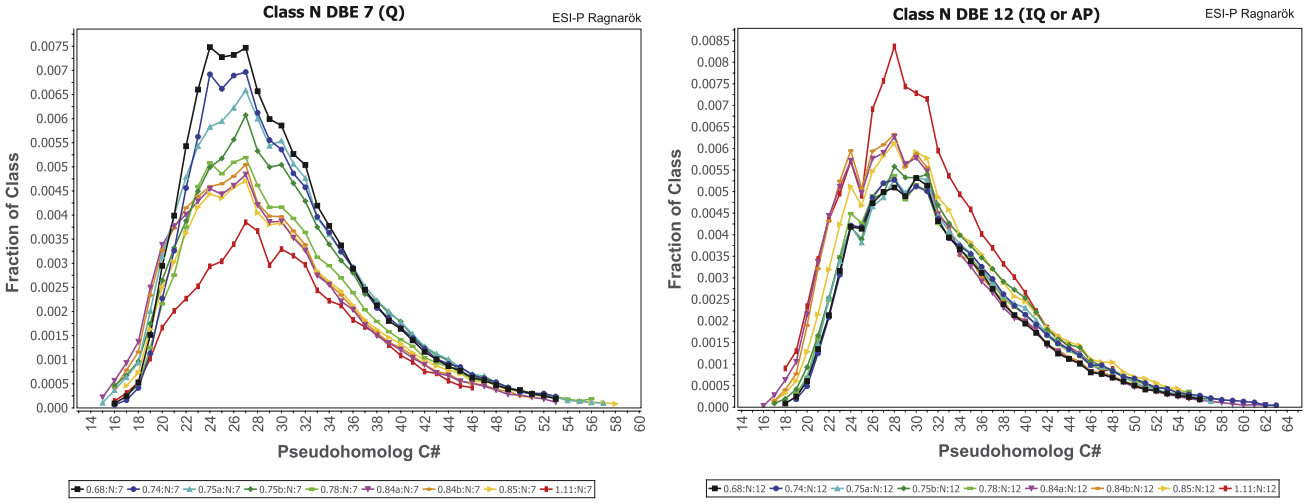

Fig. 8. Distribution of DBE 7 and DBE 12 groups in the N_1 heteroatom class (likely alkylated pyridinic compounds such as quinolines (Q) and indenoquinolines (IQ) or azopyrenes (AP), respectively), sorted by pseudohomolog C# versus the fraction of the total heteroatom class (sum of intensities of all pseudohomologs of all DBE groups is 1) represented by each DBE compound group, measured in ESI positive ion mode. The numbers in the bottom key indicate the vitrinite reflectance equivalents of the range of oils of different maturities in this sample suite.

in Fig. 3 above, an apparent relative abundance increase of the higher, benzannulated homologues with increasing oil maturity level. Furthermore, a higher apparent relative abundance of the more condensed structured DBE 12 class of compounds (likely alkylated indenoquinolines or azopyrenes), relative to dibenzoquinolines (DBE 13) in the most mature sample (1.11%Re), as paralleled in the alkylated pyrrolic species in the N_1 heteroatom class from ESI-N mode analysis was observed. Highly condensed and substantially dealkylated heteroatom compounds would appear to begin to dominate the polar fractions for very mature oils near the end of the oil window. They may thus have some utility as maturity indicators in this important maturity range, critical for shale reservoired petroleum developments.

3.4. Low polarity compound classes (measured in APPI-P mode)

All compound classes analyzed, regardless of the ionization technique used, show a strong decline in relative apparent intensity at higher oil maturity, at least for the most mature oil at 1.11 %Re. This is most likely due to the large increase in concentrations of saturated hydrocarbons (non-detectable with current FTICR-MS ionization techniques) at maturities > 1 %Re. Iatroscan (Karlsen and Later, 1991) analysis revealed that the proportion of saturated hydrocarbons in the oils increase from about 25% for the lowest maturity oil to 70% for the most mature oil (Table 2). The aromatic hydrocarbon fraction, declines from about 40% to 20% throughout the oil maturity range studied, whereas the proportion of the

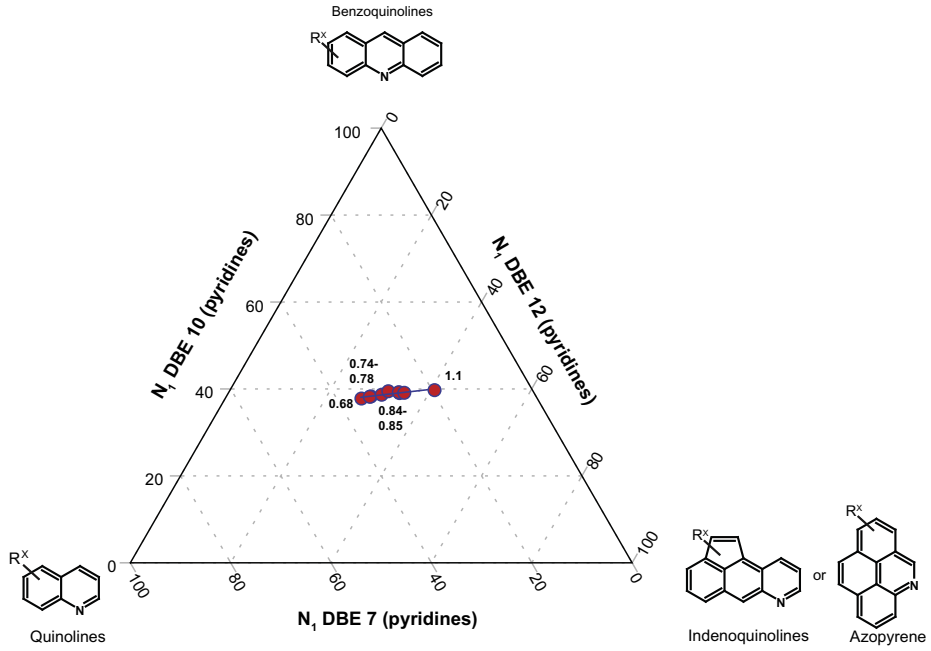

Fig. 9. Triangular plot illustrating the effect of maturity changes on the relative distribution of putative alkylated quinolines (DBE 7), benzo- (DBE 10) and indenoquinolines or azopyrenes (DBE 12). (structures only for illustration as putative generic structures); [numbers near the red data points indicate the oil maturity, assessed as vitrinite reflectance equivalent %Re; molecular structures illustrate possible core structures that correspond to a specific DBE number 7, 10, and 12, respectively.] (For interpretation of the references to color in this figure legend, the reader is referred to the web version of this article.)

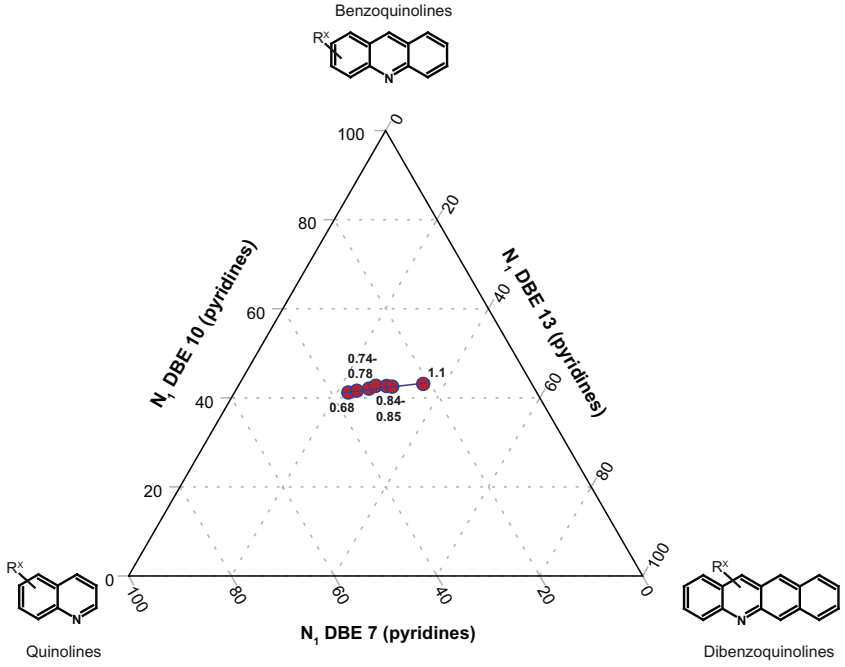

Fig. 10. Triangular plot illustrating the effect of maturity changes on the relative distribution of putative alkylated quinolines (DBE 7), benzo-(DBE10) and dibenzoquinolines (DBE 13) (structures only indicated for illustration as possible generic examples); [numbers indicate the oil maturity assessed as vitrinite reflectance equivalent %Re; molecular structures illustrate possible core structures that correspond to a specific DBE number as indicated on the triangular diagram axes].

non-hydrocarbon constituents in the oils decreased from about 35% at the beginning of the oil window (0.68 %Re) with a maximum of 45% at 0.75 %Re to around 10% at 1.11 %Re. However, within the ionizable fraction imaged using FTICR-MS in APPI-P mode, huge differences in the relative abundance of the heteroatom and hydrocarbon classes are observed with changing oil maturity. The compound class distribution patterns for the radicals and protonated low polarity pseudohomologs measured in APPI-P mode, are shown in Fig. 11. The hydrocarbon class pseudohomologs (HC) strongly increase in relative apparent abundance with increasing oil maturity level, for both the protonated and radical ions. The fraction of the hydrocarbon classes of the total ions seen in APPI-P mode, increase between the least and the most mature oil samples, for both protonated and radical hydrocarbon ions. All other detected compound classes, show a decline in relative ion abundance. Thus, for instance, the S_1 heteroatom class shows dramatic reduction in

Table 2
Percentage of the SARA fractions (saturated hydrocarbons, aromatic hydrocarbons, resins (R), asphaltenes (Asph)) of the oil samples measured by Iatroscan.

%Re	Fractions (%)				R + Asph
	Saturated HC	Aromatic HC	Resins	Asphaltenes	
0.68	24.7	39.5	32.8	3.0	35.7
0.74	20.5	38.2	36.6	4.8	41.3
0.75	25.9	28.6	34.5	11.0	45.5
0.78	29.2	37.4	25.5	8.0	33.4
0.84	33.7	38.8	24.3	3.2	28.5
0.84	36.8	34.7	26.9	1.6	27.5
0.85	38.9	34.9	23.6	2.6	25.8
1.11	69.9	19.5	10.6	0.0	10.6

relative abundance between the least and most mature oil sample and no protonated S_1 heteroatom class components could be detected in the most mature oil (Fig. 11). Furthermore, as described above, more and more heteroatom classes gradually disappear, below detection limit, with increasing oil maturity. Whereas 15 compound classes were detected in the oils in APPI-P mode at low oil maturity (ca. 0.7 %Re), only 6 compound classes (including the two non-polar hydrocarbon classes [RAD + PRO]) are left at high oil maturity (1.11 %Re).

3.5. Sulfur containing compound classes (measured in APPI-P mode)

Most of the sulfur present in crude oils and bitumens is organically bound. The abundance of these organic sulfur compounds (OSC) depends primarily on the composition of the original kerogen composition and on its maturity (Orr, 1986; Sinninghe Damsté and de Leeuw, 1990). Ho et al. (1974) subdivided the OSC in crude oils into six sulfur compound classes, namely nonthiophenic sulfur, thiophenes, benzothiophenes, dibenzothiophenes, benzonaphthothiophenes and a "sulfur not recovered" class, and classified crude oils into three "maturity groups" on the basis of the content and distribution of OSC described in this way. More recently, increasing interest has been shown in the distributions of dibenzothiophenes (DBT) and methyl dibenzothiophenes (MDBT) due to their systematic variation with increasing maturity (Radke et al., 1982; Hughes, 1984; Radke et al., 1986; Leythaeuser et al., 1988; Radke and Willsch, 1991).

The relative abundance and distribution of sulfur containing heteroatom classes (S_1, S_2 and OS), are strongly affected by the level of oil maturity. In comparison to the other heteroatom and hydrocarbon classes detected in APPI-P mode, the sulfur pseudohomologs are those most readily depleted in abundance on a relative basis, and also likely on an absolute basis, during maturity. The S_2 heteroatom class, OS heteroatom classes (both RAD + PRO), and the protonated S_1 heteroatom class were found to be in the least mature oils, but were not detectable in the most mature oil. As described above, the radical ions of the S_1 heteroatom class, as a fraction of total ions detected in APPI-P mode, decreased from about 0.18 in the low maturity oil (0.68 %Re) to only 0.01 in the most mature oil studied (1.11 %Re). The general decrease in abundance of sulfur species in crude oils with maturity is well known (Ho et al., 1974; Eglinton et al., 1990) and the FTICR-MS data are merely mirroring this well known trend, over a much broader range of sulfur-containing constituent types and molecular weights in oil than have been described before.

The embedded diagram in Fig. 11 shows a clear correlation between the reported sulfur content of the oils and the summed fraction of total ions of sulfur-containing heteroatom classes (S_1, S_2, OS as RAD and PRO ions) measured in APPI-P mode. A general positive correlation between bulk sulfur content and S_1, S_2 and NS classes (measured in APPI-P) was also previously determined using Spearman's rank correlation visualized as Circos diagrams (Hur et al., 2010).

It would appear that a representative fraction and perhaps most of the sulfur in these oils, is measured as sulfur compounds in APPI-P mode or at least that these detected sulfur-containing components are highly representative of the dominant sulfur species in the oil suite studied. In a similar manner to the principal nitrogen-containing oil constituents described in these samples (likely alkylated and highly aromatic pyridinic and pyrrolic species), reported

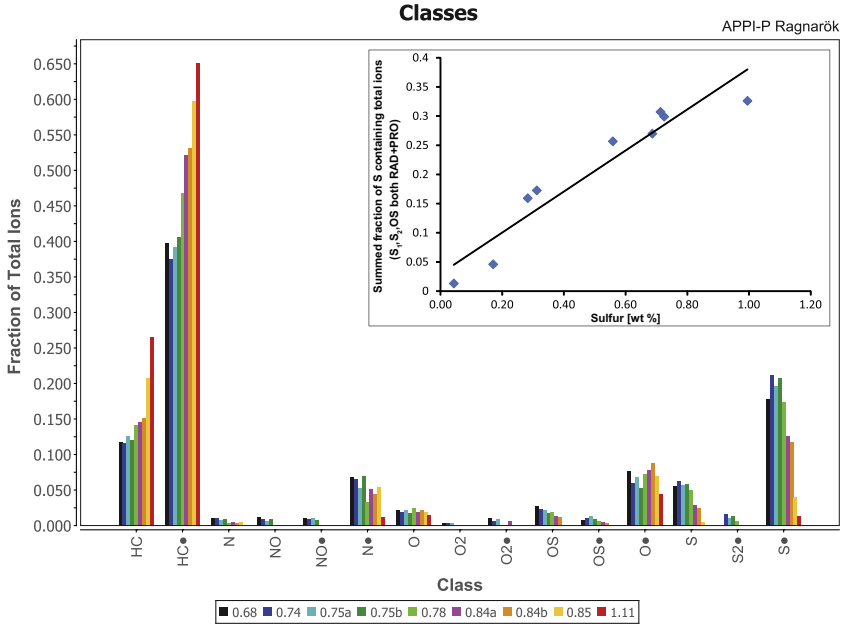

Fig. 11. Relative distribution of all heteroatom and hydrocarbon classes detected in APPI positive ion mode. The fraction of total ions is defined as the fraction of the total intensities of a compound class, normalized to the sum of the intensities of all compound classes in the samples identified with this ionization technique (i.e., sum of all classes is normalized to 1). [The dot indicates radical heteroatom or hydrocarbon classes; the other classes are found as protonated species. The numbers in the bottom key indicate the maturity levels of the oils, assessed as vitrinite reflectance equivalents-%Re. The embedded diagram shows the total sulfur content of the oils, versus the summed fraction of total ions of sulfur-containing component classes (S_1, S_2, OS as RAD and PRO ions), as measured in APPI-P mode.

above, a strong relative depletion of alkylated, aromatic sulfur compounds (S_1 RAD; thiophenic pseudohomologs), is observed with increasing oil maturity, as shown in Fig. 12. At low oil maturity, the compound class is most likely dominated by alkylbenzothiophenes (BTs; DBE 6) and to a lesser extent alkyldibenzothiophenes (DBTs; DBE 9). From 0.68–0.75 %Re, as oil maturity increases, a slight relative increase of these two pseudohomolog groups is observed, followed by a sharp decrease in relative abundance at higher maturity. By 0.85 %Re, no BTs could be detected and at 1.11 %Re all compound groups with DBE < 10, have disappeared, with only 5 DBE groups remaining (DBE groups 10–14). The observation of a trend towards dominance, on a relative basis, of higher DBE number groups of sulfur compounds with increasing oil maturity, is similar to trends found for the nitrogen compound classes described above. The embedded diagram in Fig. 12, shows the ratio of BTs/DBTs, as a function of the oil maturity, and highlights the apparent relative increase of the higher benzannulated compounds with increasing oil maturity, a common trend for all heteroatom constituents. One oil with intermediate level of maturity (0.78 %Re), shows a slightly different DBE group distribution pattern for the S_1 heteroatom class, with lower ratios of the species with DBE 6–7 and DBE 9–10. This oil seems slightly anomalous on several of the parameters, possibly suggesting oil charge contributions from a second source or a different sub-facies of the same source rock.

A comparison of FTICR-MS data for this oil suite, with quantitative GC–MS data for the alkylated dibenzothiophenic species from the current oil suite (after Bennett et al. (2002)), is shown in Fig. 13. The concentration of the non-alkylated dibenzothiophene (DBT) is typically > 200 ppm at low oil maturity levels (< 0.85 %Re), followed by a steep decline in abundance to around 35 ppm at the end of the maturity range studied. The methyldibenzothiophenes (MDBT), show a similar trend, with a slight increase in abundance, from 0.68 %Re (390 ppm) to 0.84 %Re (490 ppm), followed by a strong decrease in concentration to about 120 ppm at high oil maturity. A comparison of this quantitative GC–MS data, with the relative abundance data of the S_1 heteroatom class, DBE 9 group of compounds, accessed using FTICR-MS analysis is very encouraging for the use of FTICR-MS data in more than a qualitative way. These aromatic sulfur compounds (likely alkyldibenzothiophenes (DBTs)), show a similar trend to the GC–MS data, including a strong decrease in relative concentration, around 0.85 %Re. The most mature oil studied has essentially no detectable signal for this compound group. The embedded table in Fig. 13 shows the average molecular mass (AMM) of the S_1 heteroatom class, DBE 9 compound group, which shows a systematic decrease of ~30 Da in average molecular mass over the maturity range 0.7–0.85 %Re. The highest maturity sample had too little signal for this pseudohomolog group to produce a reliable estimate of molecular mass. Again, this contributes to the notion that a major signal seen in response to increasing oil maturity, as determined by FTICR-MS analysis, is progressive reduction in molecular size of aromatic heteroatom constituents with maturity, likely as a result of dealkylation of free species, or dilution by lower molecular weight homologs generated anew from kerogen maturation.

3.6. Hydrocarbon compound classes (measured in APPI-P mode)

The hydrocarbons (HC) seen in APPI mode, both the radical (RAD) and protonated (PRO) ion species, are the only compound classes among the FTICR-MS detectable constituents seen in this ionization mode that show a relative increase in abundance with oil maturity. Fig. 14 illustrates the strong relative increase in the apparent abundance of all DBE groups of the HC RAD class of pseudohomologs with increasing oil maturity. The overall distribution pattern seen remains similar at low oil maturity until an oil maturity of 0.84 %Re. At higher maturity, especially in most mature oil analyzed (1.11 %Re), a change in the distribution pattern of hydrocarbons occurs, mainly as an addition of new species appearing in the low DBE range of DBE 4–7. This might be an indication of an addition of 1- and 2-ring aromatic and mixed saturated and aromatic hydrocarbons generated from larger heteroatom constituents in the source organic matter or reservoir. Unfortunately, a mass balance to further test this notion is currently not possible

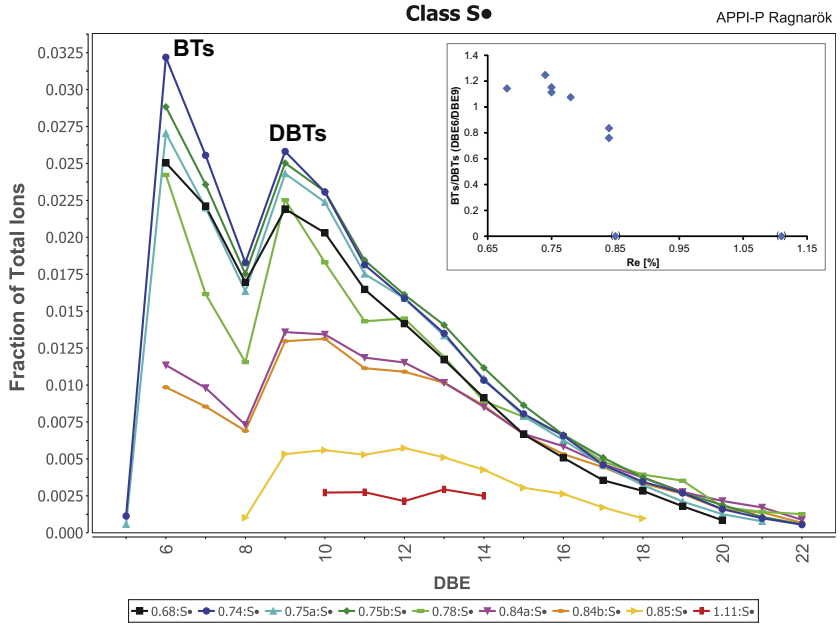

Fig. 12. Distribution of S_1-heteroatom class, sorted into groups of double bond equivalents (DBE), plotted versus relative abundance of each DBE group, measured in APPI positive ion mode. DBE 6 group components are likely derivatives of alkylated benzothiophenes (BTs) and DBE 9 group pseudohomologs are likely derivatives of alkylated dibenzothiophenes (DBTs). The embedded smaller diagram shows the ratio of the relative abundances of pseudohomologs with DBE 6, to compounds with DBE 9 constituents, (the putative ratio of alkylated benzothiophenes to alkylated dibenzothiophenes) versus oil maturity. The numbers in the bottom key indicate the maturities of the different oils, assessed in terms of vitrinite reflectance equivalent-%Re.

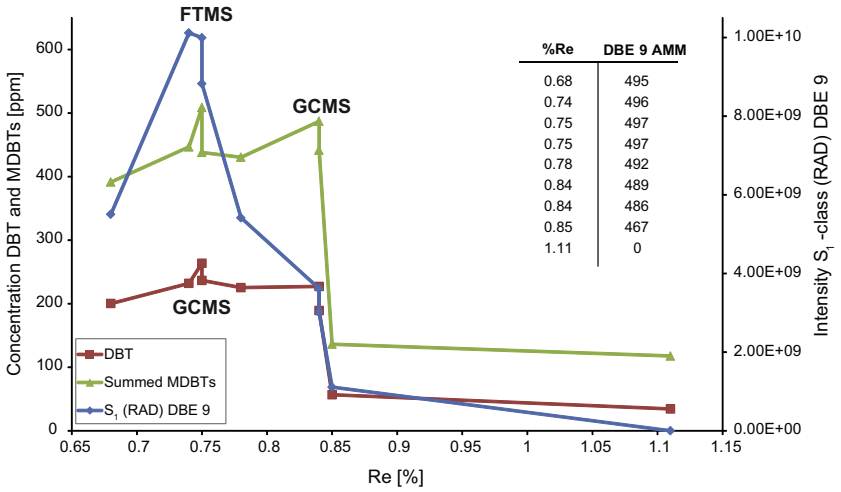

Fig. 13. The absolute concentrations of dibenzothiophene and summed methyldibenzothiophenes measured by GC MS (courtesy of Bennett et al. (2002)) and the relative abundance of S_1 class DBE 9 group compounds (likely, alkylated dibenzothiophenes-DBTs), analyzed in APPI-P mode by FT-ICR-MS. The embedded table shows the average molecular mass (AMM) of the S_1 class DBE 9 group for the oil maturity suite.

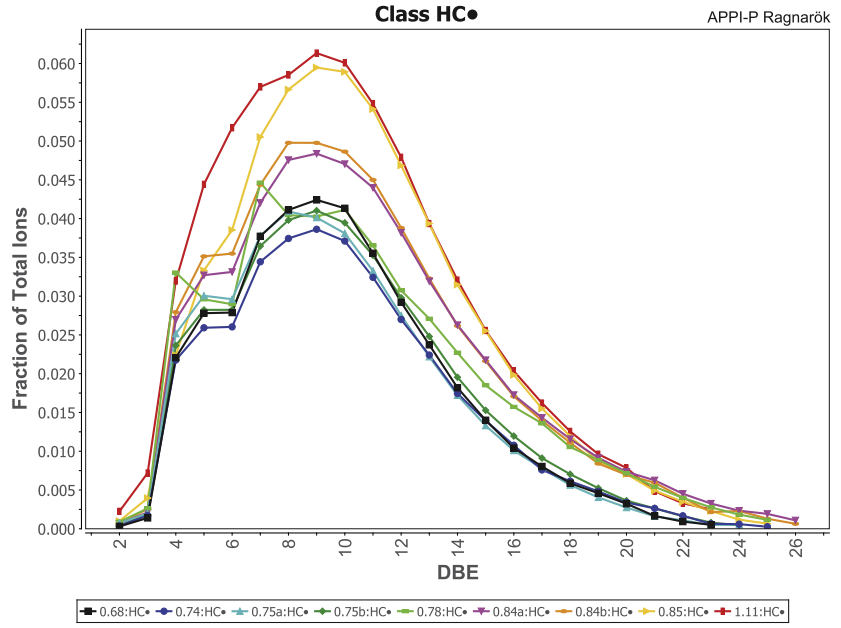

Fig. 14. Distribution of HC class (radical ions) for the oil suite, sorted by groups of double bond equivalents (DBE), plotted versus the relative abundance of pseudohomologs within each DBE group, measured in APPI positive ion mode. Fraction of total ions is defined as the abundance measured as the sum of abundances of all components within one DBE group of a compound class normalized to the sum of all assigned peaks in a sample reported in APPI-P ion mode. The numbers in the bottom key indicate the vitrinite reflectance equivalents of the range of oils of different maturities.

as it would need to include quantitative analysis of heteroatom classes measured with different ionization techniques. The distribution pattern of one slightly anomalous oil with intermediate maturity levels (0.78 %Re) again shows an exception, with higher concentrations of pseudohomolog groups with DBE 4, 7 and 10, these most likely being groups dominated by alkylated benzenes, naphthalenes and phenanthrenes, respectively. Overall, however, there are very consistent trends in the behavior of the hydrocarbon radical class species, which all increase in relative abundance in a systematic manner.

The distribution pattern of the protonated hydrocarbons class (HC PRO) of the maturity suite is shown in Fig. 15A. Similar to the radical ions data, a relative increase in abundance is observed throughout the maturity sequence, with a predominance of constituents within the DBE 6 group. Apart from the unusual oil with intermediate maturity (0.78 %Re), only the highest maturity oil sample studied differs from the general distribution pattern seen in the other oils, in essence having a predominance of pseudohomologs within the hydrocarbon class at DBE 5. This group of compounds is currently unidentified, but is likely to be hopanes, alkylated tetralins and/or diamantanes, cage-like hydrocarbons which are known to be thermally stable and commonly enriched in high maturity oils (Peters et al., 2005). Whereas alkylated tetralins, as aromatic compounds would be expected to produce more radical ions (HC RAD), it is less clear if saturated cyclic and highly branched compounds can readily ionize under these conditions. We do see that hydrocarbons such as steranes do in fact ionize in this way and thus we would expect hopanes to behave similarly. We have no direct evidence that alkylated diamondoid hydrocarbons can ionize under these conditions in our lab and in fact

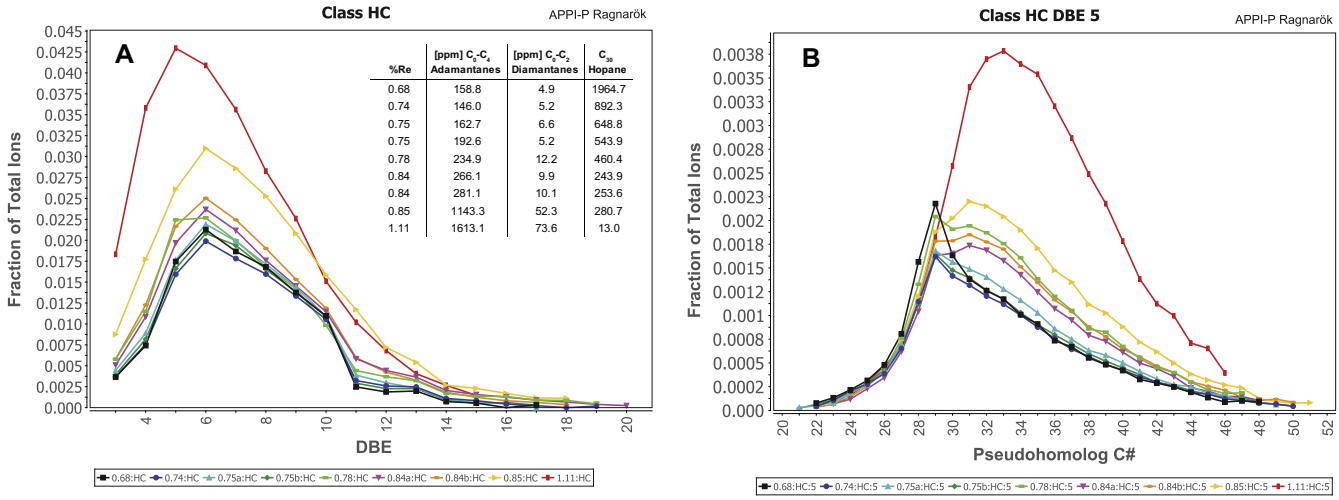

Fig. 15. (A) Distribution of HC class pseudohomologs (protonated ions), sorted by groups of double bond equivalents (DBE), plotted versus their relative abundance as measured in APPI positive ion FTICR-MS mode. The embedded table shows the concentrations of the C_{30} hopane, C_{0-4} adamantanes and C_{0-2} diamantanes for the maturity suite measured by GC-MS. (B) Distribution of HC class pseudohomologs (protonated ions), DBE 5 group compounds, sorted by pseudohomolog C# and plotted versus their relative abundance as measured in APPI positive ion mode. The fraction of total ions is defined as the fraction of the total intensities of the DBE group of components, in a particular hydrocarbon class (RAD or PRO), normalized to the sum of the intensities of all compound classes identified with this ionization technique (sum of all hydrocarbon and heteroatom classes is normalized to 1). The numbers in the bottom key indicate the maturity level of the oils, assessed as vitrinite reflectance equivalents (%Re).

adamantanes do not ionize but the literature suggests that ionization of the higher diamondoids may in fact occur (Lenzke et al., 2007). In addition, the ionization energy decreases with increasing alkylation (Hanley and Zimmermann, 2009). Further study, of course, would be necessary to verify such inferences. The embedded table in Fig. 15A shows quantified GC–MS data for the C_{30} hopane, C_{0-4} adamantanes and C_{0-2} diamantanes for this oil suite. The C_{30} hopane is representative of the whole hopane group of compounds, which all showed a similar trend of a strong decrease in concentration with increasing oil maturity, with one order of magnitude reduction in concentration by a maturity level of 0.85 %Re and another order of magnitude reduction in concentration by 1.11 %Re (after Bennett et al., 2002). Simultaneously, diamantanes (C_{0-2}) show a strong increase in abundance as oil maturity increases (concentrations of these compounds increase by more than one order of magnitude over the range of maturity studied). The relative abundances of the DBE 5 pseudohomologs as a function of carbon number as recorded by FTICR-MS analysis, are shown in Fig. 15B. At low oil maturity, compounds in the range of C_{28}–C_{35} are the most abundant on a relative basis, which might plausibly reflect pentacyclic triterpanes such as hopanes. At high oil maturity the distribution pattern shifts to higher carbon numbers, peaking at C_{33}. This might indicate an increase in highly alkylated diamantanes whereas the concentrations of the hopanes are becoming less predominant. Highly alkylated diamantanes with carbon numbers up into the C_{40} range and above, are not described in the literature yet, due to the technical limits of GC–MS. Clearly, while much additional work, with standards and other analytical methods, would be needed to verify the identity of the species, it is clear FTICR-MS is a powerful reconnaissance tool for the identification of components that may be valuable additional elements in the arsenal of the petroleum geochemist.

4. Summary

A suite of closely related oils, with the same clastic marine source rock characteristics, but with different levels of thermal maturity, were analyzed with a 12 T ultra-high resolution mass spectrometer (FTICR-MS), to investigate the compositional changes in the polar oil constituents, as a function of oil maturity. While one oil in this set, appeared to have slightly different source characteristics, overall, a clear trend in composition versus oil maturity level was evident in several sets of parameters. Encouragingly, while the actual identities of many of the chemical species detected using FTICR-MS cannot be directly verified from FTIRC-MS data alone, close covariation between the behavior of several nitrogen (e.g. carbazole family compounds), and sulfur (e.g. dibenzothiophene family compounds), species where both GC–MS data and inferred identity using FTICR-MS data were available on the same samples, suggests that FTICR-MS does appear to have some rudimentary quantitation capability. Additionally, this covariation strongly supports the tentative identification of some of the compound speciations discussed in the text. Increasing oil maturity level had a strong influence on the composition of all compound classes in the oils but several major observations are clearly evident.

The relative apparent abundances of all heteroatom classes detected in this study using both ESI-N, ESI-P and APPI ionization modes, decrease systematically with increasing oil maturation levels. This is likely due to a strong increase in the absolute concentration of non-detectable hydrocarbons in the crude oils with increasing maturity level.

Both aromatic hydrocarbons (detectable in APPI mode) and heteroatom classes (detectable in both ESI and APPI modes), as broad classes, are becoming more aromatic (shift to a greater predominance of higher DBE group members) and dealkylated (decreasing average molecular mass of individual pseudohomolog groups), with increasing maturation level in the oil suite. This is true for essentially all compound types.

Several putative oil maturity level dependent molecular ratios were identified in the study. Of particular note, the relative abundance ratios of heteroatom classes such as putative alkylated carbazoles, quinolines and benzothiophenes, compared to their benzannulated homologs are very sensitive to maturation level and could become useful novel maturity proxies. At higher molecular weight, such proxy ratios could be quite advantageous in the maturity assessment of heavily or severely biodegraded crude oils, as it would be predicted that high molecular weight heteroatom aromatic compounds would be highly resistant to biodegradation.

While not yet quantitative, FTICR-MS allows us to analyze a much broader range of oil constituents than current GC–MS does and undoubtedly adds much useful information on compositional

changes in the nonhydrocarbon and high molecular weight aromatic hydrocarbon species present in maturing crude oils. Encouragingly, covariation of GC–MS data for alkylated, aromatic sulfur- and nitrogen-containing compounds in this oil suite, with the corresponding FTICR-MS data from compounds inferred to be alkylated sulfur and alkylated nitrogen constituents is very strong encouragement to persist with attempts to make Fourier transform mass spectrometry as quantitative as it can be. Clearly, FTICR-MS already has some very rudimentary quantitation capabilities.

As FTICR-MS technology becomes more readily usable in non-specialist laboratories, it is likely that maturity and source facies parameters based on FTICR-MS data will begin to be tested in field applications.

Acknowledgements

We thank the FTICR-MS project consortium at PRG (Ecopetrol, Petrobras and Shell International) for their financial support and permission for publication. Aphorist Inc. is thanked for providing access to the FTICR-MS data analysis and visualization software Ragnarök. Bruker are thanked for their continued support, in the development of the University of Calgary FTICR-MS facility. Comments and suggestions from Clifford Walters and two unknown reviewers were very useful and are much appreciated. In addition, we would like to thank NSERC (Canada), the Canadian Foundation for Innovation (CFI) and the Canada Research Chairs for research funding.

Appendix A

A brief summary of typical heteroatom classes and more speculatively, component functional groups detectable with the different ionization techniques are as follows:

The ESI-N (negative ion mode), technique allows the optimal detection and monitoring of acidic compounds, i.e. compounds which are able to deprotonate such as compounds, including carboxylic acids, alcohols, pyrroles (Qian et al., 2001a).

The ESI-P (positive ion mode), technique allows the detection of basic compounds, i.e. compounds which can be readily protonated; for example compounds with pyridinic nitrogen groups (Qian et al., 2001b).

The APPI-P technique allows the detection of analyte components as protonated (PRO) and/or radical (RAD) ion species. What ions are formed depends on the proton and electron affinities of the dopant relative to the analyte. With a toluene dopant, if the proton affinity of the analyte is higher than the proton affinity of the benzyl radical, a protonated molecule can form. If the electron affinity of the toluene radical cation is higher than the electron affinity of the analyte (lower or equal ionization energy than toluene) a radical molecular ion can form (Purcell et al., 2006). Compounds containing one or more aromatic rings are detectable by this technique, which are not efficiently ionized by ESI (e.g. alkylated aromatic hydrocarbons and thiophenic species).

A.1. Data illustrations

A.1.1. Definition of oil constituent species

A (heteroatom or hydrocarbon) class is defined here as the sum of all constituents containing the same heteroatoms (number and elements) independent of the degree of unsaturation (DBE). These would be measured in one ionization technique mode (ESI-N, ESI-P or APPI-P; radical ions (RAD) and protonated ions (PRO) of one heteroatom or hydrocarbon class in APPI-P are considered as two classes).

A DBE group of compounds is defined as the sum of all constituents containing the same heteroatoms (number and elements) and double bond equivalent number measured in one ionization technique mode.

A pseudohomolog at a specific carbon number (C#), of a species is defined as the sum of all compounds containing the same molecular formula measured in one ionization technique mode.

Note: A DBE group of compounds would be recognized by the interpreter as having an acceptable signal-to-noise ratio, within any ionization mode, if the pseudohomolog distribution at that DBE group number, showed a minimum of five consecutive pseudo-homologues with Gaussian shaped peak distribution easily recognizable above the noise.

The different plot types used in this article are briefly explained below.

A.1.2. Bar and line plots

'Ion Intensity' versus pseudohomolog ($C^{\#}$), DBE group or distribution of heteroatom and hydrocarbon classes plots:

An ion intensity plot represents the absolute ion intensity, measured in a single ionization mode, of either the response of a pseudohomolog at one carbon number: the response of a DBE group of compounds within one heteroatom (or hydrocarbon) class: or the distribution of a heteroatom (or hydrocarbon) class in total. Commonly, we plot the absolute ion intensity of all pseudohomologs; all DBE groups; or all heteroatom (or hydrocarbon) classes on one diagram against absolute ion intensity measured in that single ionization mode.

This plot allows a tentative estimation of the relative concentration and variation between samples, of different constituents (acidic moieties in ESI-N; basic moieties in ESI-P; low polarity species to non-polar species in APPI-P) in the oil sample, as in all cases, and for comparative purposes, the whole oil samples (without any prior separation) are analyzed under identical conditions.

'Fraction of Total Ions' versus distribution of a compound class, DBE group or pseudohomolog ($C^{\#}$) plots:

A *'Fraction of Total Ions'* plot is simply an ion intensity plot, for a heteroatom (or hydrocarbon) class, a DBE group of compounds, or for pseudohomologs at one or more carbon numbers, where the ion counts for each species group are now normalized to the total ion response of the entire sample analyzed in one ionization mode.

'Fraction of Class' versus distribution of compound class, DBE or pseudohomolog C# plots:

A *'Fraction of Class'* plot is simply a heteroatom (or hydrocarbon) class specific plot, whereby the ion intensities for a DBE group of compounds or for pseudohomologs at one or more carbon numbers, are now normalized to the total ion response of the heteroatom (or hydrocarbon) class analyzed in one ionization mode.

A.1.3. Modified Kendrick plot

The 'Modified Kendrick plot' illustrates the distribution of all components within a heteroatom compound class (analyzed with any ionization technique), as a plot of C# versus DBE with the intensity of the component being reflected by a color code. The colors reflect the peak intensity of individual carbon number components, relative to the most intense peak within the overall compound class.

A.1.4. Average molecular mass

The average molecular mass (AMM) plot shows the averaged molecular mass of all components in an individual DBE group of compounds from a heteroatom (or hydrocarbon) class, plotted as a function of the DBE number. The AMM is defined as: AMM = Σ intensity of each individual pseudohomolog * accurate mass of the pseudohomolog/total ion intensity for all pseudohomologs within a DBE group of compounds.

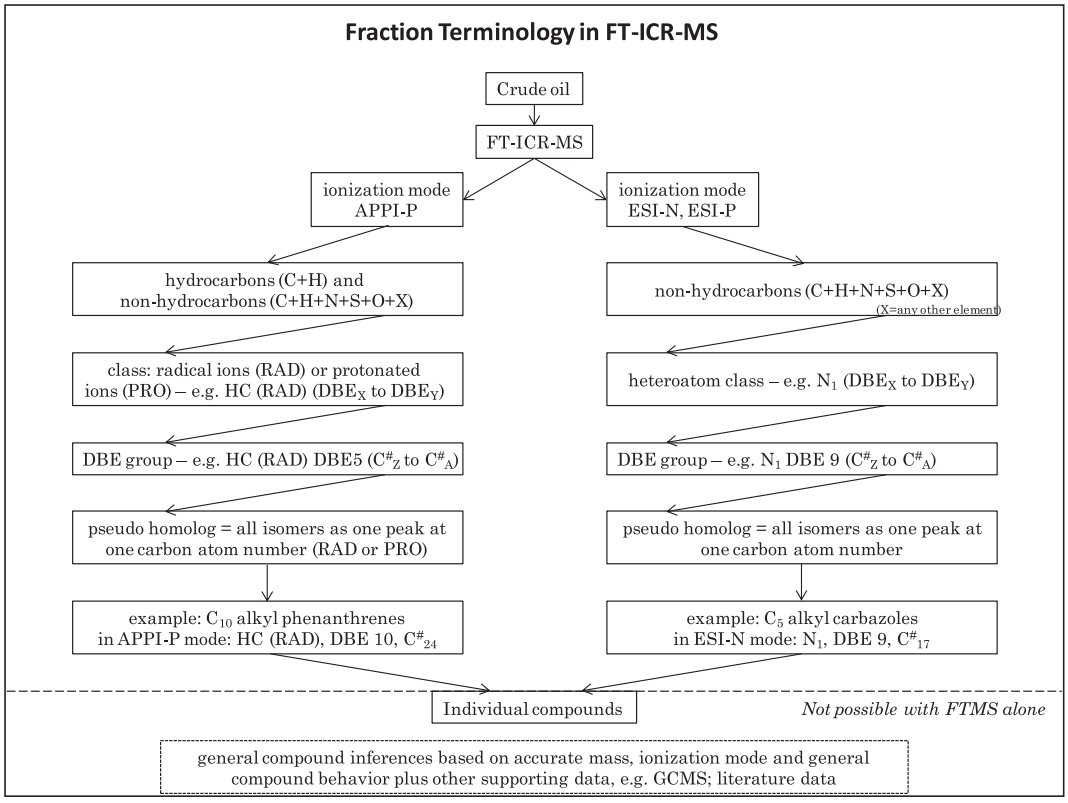

Associate Editor—**Clifford C. Walters**

References

Ball, J.S., 1962. Nitrogen compounds in petroleum. ACS Division of Science and Technology 42, 27–30.

Bechtel, A., Gratzer, R., Linzer, H.-G., Sachsenhofer, R.F., 2013. Influence of migration distance, maturity and facies on the stable isotopic composition of alkanes and on carbazole distributions in oils and source rocks of the Alpine Foreland Basin of Austria. Organic Geochemistry 62, 74–85.

Bennett, B., Chen, M., Brincat, D., Gelin, F.J.P., Larter, S.R., 2002. Fractionation of benzocarbazoles between source rocks and petroleums. Organic Geochemistry 33, 545–559.

Clegg, H., Wilkes, H., Oldenburg, T., Santamaria-Orozco, D., Horsfield, B., 1998. Influence of maturity on carbazole and benzocarbazole distributions in crude oils and source rocks from the Sonda de Campeche, Gulf of Mexico. Organic Geochemistry 29, 183–194.

Eglinton, T.I., Sinninghe Damste, J.S., Kohnen, M., de Leeuw, J.W., Larter, S.R., Patience, R.L., 1990. Analysis of maturity-related changes in the organic sulfur composition of kerogens by flash pyrolysis-gas chromatography. American Chemical Society Symposium Series 429, 529–565.

Frolov, Y.B., Smirnov, M.B., Vanyukova, N.A., Sanin, P.I., 1989. Carbazoles of crude oil. Petroleum Chemistry USSR 29, 87–102.

Hanley, L., Zimmermann, R., 2009. Light and molecular ions: the emergence of vacuum UV single-photon ionization in MS. Analytical Chemistry 81, 4174–4182.

Helm, R.V., Latham, D.R., Ferrin, C.R., Ball, J.S., 1960. Identification of carbazole in Wilmington petroleum through use of gas liquid chromatography and spectroscopy. Analytical Chemistry 32, 1765–1767.

Hesse, M., 1974. Indolalkaloids. In: Budzikiewicz, H. (Ed.), Progress in Mass Spectrometry, vol. 1. Verlag Chemie, Weinheim, pp. 165–189.

Ho, T.Y., Rogers, M.A., Drushel, H.V., Koons, C.B., 1974. Evolution of sulphur compounds in crude oils. AAPG Bulletin 58, 2338–2348.

Huang, H., Bowler, B.F.J., Zhang, Z., Oldenburg, T.B.P., Larter, S.R., 2003. Influence of biodegradation on carbazole and benzocarbazole distributions in oil columns from the Liaohe basin, NE China. Organic Geochemistry 34, 951–969.

Hughes, W.B., 1984. Use of thiophenic organosulphur compounds in characterizing crude oils derived from carbonate versus siliciclastic sources. In: Palacas, J.G. (Ed.), Petroleum Geochemistry and Source Rock Potential of Carbonate Rocks, vol. 18. American Association of Petroleum Geologists, Tusla, pp. 181–196.

Hughey, C.A., Rodgers, R.P., Marshall, A.G., Walters, C.C., Qian, K., Mankiewicz, P., 2004. Acidic and neutral polar NSO compounds in Smackover oils of different thermal maturity revealed by electrospray high field Fourier transform ion cyclotron resonance mass spectrometry. Organic Geochemistry 35, 863–880.

Hunt, J.M., 1995. Petroleum Geochemistry and Geology. W.H. Freeman & Company, San Francisco.

Hur, M., Yeo, I., Kim, E., No, M., Koh, J., Cho, Y.J., Lee, J.W., Kim, S., 2010. Correlation of FT-ICR mass spectrometry with the chemical and physical properties of associated crude oils. Energy & Fuels 24, 5524–5532.

Karlsen, D.A., Larter, S.R., 1991. Analysis of petroleum fractions by TLC-FID – applications to petroleum reservoir description. Organic Geochemistry 17, 603–617.

Larter, S.R., Bowler, B.F.J., Li, M., Chen, M., Brincat, D., Bennett, B., Noke, K., Donohoe, P., Simmons, D., Kohnen, M., Allan, J., Telnæs, N., Horstad, I., 1996. Molecular indicators of secondary oil migration distances. Nature 383, 593–597.

Larter, S.R., Head, I.M., Bennett, B., Huang, H., Adams, J.J., Oldenburg, T.B.P., Marcano, N., 2013. The Roles of Water in Subsurface Petroleum Biodegradation – Part 1 the Role of Water Radiolysis. Abstract, CSPG Geoconvention ''Integration'', Calgary, Alberta, Canada.

Lenzke, K., Landt, L., Hoener, M., Thomas, H., Dahl, J.E., Liu, S.G., Carlson, R.M.K., Müller, T., Bostedt, C., 2007. Experimental determination of the ionization potentials of the first five members of the nanodiamond series. The Journal of Chemical Physics 127, 084320.

Leythaeuser, D., Radke, M., Willsch, H., 1988. Geochemical effects of primary migration of petroleum in Kimmeridge source rocks from Brae field area, North Sea. II: Molecular composition of alkylated naphthalenes, phenanthrenes, benzo- and dibenzothiophenes. Geochimica et Cosmochimica Acta 52, 2879–2891.

Li, M.W., Larter, S.R., Stoddart, D., Bjoroy, M., 1992. Liquid-chromatographic separation schemes for pyrrole and pyridine nitrogen aromatic heterocycle fractions from crude oils suitable for rapid characterization of geochemical samples. Analytical Chemistry 64, 1337–1344.

Mackenzie, A.S., Brassell, S.C., Eglington, G., Maxwell, J.R., 1982. Chemical fossils: the geological fate of steroids. Science 217, 491–504.

Marshall, A.G., Rodgers, R.P., 2004. Petroleomics: the next grant challenge for chemical analysis. Accounts of Chemical Research 37, 53–59.

Newkome, G.R., 2008. The Chemistry of Heterocyclic Compounds: Pyridine and its Derivatives. Part 5, vol. 14. John Wiley & Sons.

Oldenburg, T.B.P., 2004. Geochemical Significance of Heterocompounds in Petroleum Systems, Offshore Norway, 2004. Jülich-Oldenburg, PhD Thesis.

Oldenburg, T.B.P., Huang, H., Donohoe, P., Willsch, H., Larter, S.R., 2004. High molecular weight aromatic nitrogen and other novel hopanoid-related compounds in crude oils. Organic Geochemistry 35, 665–678.

Oldenburg, T.B.P., Larter, S.R., Huang, H., 2006. Nutrient supply during subsurface oil biodegradation – availability of petroleum nitrogen as a nutrient source for subsurface microbial activity. Energy & Fuels 20, 2079–2082.

Oldenburg, T.B.P., Larter, S.R., Huang, H., 2007. Nitrogen isotope systematics of petroleum fractions of differing polarity – neutral versus basic compounds. Organic Geochemistry 38, 1789–1794.

Oldenburg, T.B.P., Brown, M., Chanthamontri, K., Sanguantrakun, N., Bennett, B., Snowdon, R.W., Larter, S., 2013. The Controls on the Composition of Biodegraded Oils in the Deep Subsurface Part 4. Degradation and Production of High Molecular Weight Aromatic and Polar Species During In-reservoir Biodegradation. Abstract, 26th International Meeting on Organic Geochemistry, IMOG, Costa Adeje – Tenerife, Canary Islands, OP7-2.

Orr, W.L., 1986. Kerogen/asphaltene/sulphur relationships in sulphur-rich Monterey oils. In: Leythaeuser, D., Ruellkotter, J. (Eds.), Advances in Organic Geochemistry, vols. 1–3. Pergamon, Oxford-New York, pp. 499–516.

Patience, R.L., Baxby, M., Bartle, K.D., Perry, D.L., Rees, A.G.W., Rowland, S.J., 1992. The functionality of organic nitrogen in some recent sediments from the Peru upwelling region. Organic Geochemistry 18, 161–169.

Pepper, A.S., Corvi, P.J., 2005. Simple kinetic models of petroleum formation. Marine and Petroleum Geology 12, 417–452.

Peters, K.E., Walters, C.C., Moldowan, J.M., 2005. The Biomarker Guide, vol. 1. Cambridge University Press, Cambridge, United Kingdom.

Purcell, J.M., Hendrickson, C.L., Rodgers, R.P., Marshall, A.G., 2006. Atmospheric pressure photoionization Fourier transform ion cyclotron resonance mass spectrometry for complex mixture analysis. Analytical Chemistry 78, 5906–5912.

Qian, K.N., Robbins, W.K., Hughey, C.A., Cooper, H.J., Rodgers, R.P., Marshall, A.G., 2001a. Resolution and identification of elemental compositions for more than 3000 crude acids in heavy petroleum by negative-ion microelectrospray high-field Fourier transform ion cyclotron resonance mass spectrometry. Energy and Fuels 15, 1505–1511.

Qian, K., Rodgers, R.P., Hendrickson, C.L., Emmett, M.R., Marshall, A.G., 2001b. Reading chemical fine print: resolution and identification of 3000 nitrogen-containing aromatic compounds from a single electrospray ionization Fourier transform ion cyclotron resonance mass spectrum of heavy petroleum crude oil. Energy and Fuels 15, 492–498.

Radke, M., Willsch, H., 1991. Occurence and thermal evolution of methylated benzo- and dibenzothiophenes in petroleum source rocks of western Germany. In: Manning, D. (Ed.), Organic Geochemiostry. Advances and Applications in Energy and the Natural Environment. Manchester University Press, Manchester, pp. 480–484.

Radke, M., Welte, D.H., Willsch, H., 1982. Geochemical study on a well in the Western Canada Basin: relation of the aromatic distribution pattern to maturity of organic matter. Geochimica et Cosmochimica Acta 46, 1–10.

Radke, M., Welte, D.H., Willsch, H., 1986. Maturity parameters based on aromatic hydrocarbons: influence of the organic matter type. Organic Geochemistry 10, 51–63.

Sinninghe Damsté, J.S., de Leeuw, J.W., 1990. Analysis, structure and geochemical significance of organically-bound sulphur in the geosphere: state of the art and future research. Organic Geochemistry 16, 1077–1101.

Snyder, L.R., 1965. Distribution of benzocarbazole isomers in petroleum as evidence for their biogenic origin. Nature 205, 277.

Snyder, L., 1970. Petroleum nitrogen compounds and oxygen compounds. Accounts of Chemical Research 3, 290–299.

Tissot, B.P., Welte, D.H., 1984. Petroleum Formation and Occurrence. Springer Verlag, Heidelberg.

Wilhelms, A., Larter, S.R., 1994. Origin of tar mats in petroleum reservoirs. 1. Introduction and case studies. Marine and Petroleum Geology 11, 418–441.